Journal of Vibration Engineering & Technologies (2022) 10:2765–2797
https://doi.org/10.1007/s42417-022-00519-7

ORIGINAL PAPER

Free Transverse Vibration of General Power-Law NAFG Beams with Tip Masses

Mohsen Bambaeechee[1]

Received: 9 September 2021 / Revised: 14 March 2022 / Accepted: 10 April 2022 / Published online: 30 April 2022

Abstract

Purpose The present study aims to obtain the exact solutions of the free transverse vibration of non-uniform axially functionally graded (NAFG) beams with end point masses and general boundary conditions. Also, the effects of the attached end point masses, rotational and translational elastic supports, and NAFG parameters on the natural frequencies of the power-law NAFG beams are investigated.

Methods Based on the Euler–Bernoulli beam theory, the governing differential equation of motion was solved accurately using the Bessel functions. Then, the constant coefficients matrices of the power-law NAFG beams with the end point masses and general elastic supports were derived by applying the boundary conditions. The general elastic boundary conditions are modeled with the linear rotational and lateral translational springs. Furthermore, the material and geometrical properties of the NAFG beams are assumed to change continuously and together in the axial direction according to the power-law forms. By taking the constant coefficients matrix determinant equal to zero and calculating the positive real roots, the natural frequencies were obtained. By comparing the responses of the numerical examples with the available solutions, the accuracy and ability of the proposed formulations are demonstrated.

Results and Conclusion Obtained results show the natural frequencies of the power-law NAFG beam decrease with the increase of the mass ratio and increase with the increase of the stiffness ratios of the supports. Moreover, the natural frequencies of the power-law NAFG beam increase with the increase of NAFG parameters. Depending on the boundary conditions, the mass sensitivity differs from one power-law NAFG beam to another, and from one mode of vibration to another. The exact analytical solutions are listed in tabular and graphical forms and can be used as the benchmark solutions. Moreover, the results presented here can be used for the proper design of composite beams carrying end point masses with different elastic boundary conditions.

Keywords Non-uniform axially functionally graded (NAFG) beam · Tip mass · Boundary conditions · Natural frequencies · Transverse vibration · Euler–Bernoulli beam

Introduction

Beams with a non-uniform and continuous distribution of material and geometrical parameters along the axial direction, namely, non-uniform axially functionally graded (NAFG) beams due to thermal resistance, high stiffness, economic issues, and optimal design are widely utilized in many aerospace, mechanical, electrical, and civil engineering structures. Nevertheless, the non-uniform homogenous beams, i.e., tapered, wedged, stepped, and non-prismatic beams can be considered as the special case of the NAFG beams with constant material and variable geometry [1]. On the other hand, it is important to know the effect of the attached masses on the dynamic behavior and natural frequencies of the NAFG beams, to achieve the proper design of the composite structure. Accordingly, this paper is focused on the free vibration of non-uniform and NAFG beams with attached masses. So far, many reports have been published in these two areas.

About the vibration of non-uniform beams with attached masses, for the first time, Mabie and Rogers [2, 3] derived the exact analytical solutions for the transverse

✉ Mohsen Bambaeechee
m.bambaeechee@qiet.ac.ir

[1] Department of Civil Engineering, Faculty of Engineering, Quchan University of Technology, P. O. Box. 94771-67335, Quchan, Iran

vibrations of tapered and double-tapered cantilever beams with end mass. Based on the finite-element method, the transverse vibration frequencies of a linear tapered beam with one end rotational spring-hinged and carrying a mass at the other free end were studied by Sankaran et al. [4]. Using the analytical approach, Goel [5] investigated the transverse vibrations of the same beam. The closed-form solution in terms of the Bessel functions for the transverse vibrations of a tapered beam carrying a concentrated mass was obtained by Lee [6]. Lau [7, 8] analyzed the first five natural frequencies of non-uniform cantilever beams with a mass at the free end. Utilizing the Rayleigh–Schmidt approach, the fundamental mode of vibration for an elastically restrained cantilever beam with variable cross-section and tip mass was investigated by Laura and Gutierrez [9]. Alvarez et al. [10] obtained an approximate solution for the vibrations of an elastically restrained, non-uniform beam with translational and rotational springs, and with a tip mass using the optimized Rayleigh–Ritz approach. Based on the Bessel functions, the natural frequencies of the same beam were calculated by Yang [11]. An exact analytical solution for the transverse vibrations of a Timoshenko beam of non-uniform thickness clamped at one end and carrying a concentrated mass at the other was presented by Rossi et al. [12]. Lee and Lin [13] derived the exact vibration solutions for non-uniform Timoshenko beams with attachments using the power series method. Utilizing the numerical integration, an approximate method for the vibration analysis of a non-uniform Timoshenko beam with constraint at any point and carrying a heavy tip body was proposed by Matsuda et al. [14]. Based on the characteristics orthogonal polynomials method and the modified Rayleigh–Schmidt method, Grossi et al.[15] studied the vibration of tapered beams with one end spring-hinged and the other end with tip mass. An exact analysis for the transverse vibrations of a linearly tapered cantilever beam with tip mass of rotary inertia, eccentricity, and constraining springs via the Bessel functions was presented by Auciello [16, 17]. Using the same method and Rayleigh–Ritz approach, Auciello and Maurizi [18] investigated the first five natural frequencies of tapered beams with attached mass and inertia elements. The vibrations of a cantilever tapered beam with varying section properties and materials and carrying a mass at the free end utilizing the Bessel functions and Rayleigh–Ritz method were studied by Auciello and Nolè [19]. Wu and Hsieh [20] determined the natural frequencies and corresponding mode shapes of a non-uniform beam carrying multiple point masses using the analytical and numerical combined methods. Using the fundamental solutions and recurrence formulas, a new exact approach for determining the natural frequencies and mode shapes of multistep non-uniform beams with classical and non-classical boundary conditions and concentrated masses was presented by Li [21, 22]. The exact solutions for the natural frequencies and mode shapes of non-uniform beams with multiple spring-mass systems using the numerical assembly method and Bessel functions were performed by Chen and Wu [23]. Karami et al. [24] proposed a differential quadrature element method for the free vibration analysis of arbitrary non-uniform Timoshenko beams with attachments and general boundary conditions. Based on the analytical and numerical combined method, the bending vibrations of wedge beams with any number of point masses were investigated by Wu and Chen [25]. Using a similar approach, Wu and Chiang [26] studied the free vibrations of solid and hollow wedge beams with rectangular or circular cross sections and carrying any number of point masses. Exact free vibration analysis of Euler–Bernoulli tapered beams in the presence of concentrated tip mass and linear dashpot damper in terms of Bessel functions was presented by De Rosa and Maurizi [27]. Wu and Chen [28] obtained an exact solution for the natural frequencies and mode shapes of an immersed elastically restrained wedge beam carrying an eccentric tip mass with the mass moment of inertia. The free and forced vibrations of a tapered cantilever beam carrying multiple point masses were performed by Chen and Liu [29]. Based on the Adomian modified decomposition method, Lai et al. [30] investigated the free vibration of non-uniform Euler–Bernoulli beams with tip mass of rotatory inertia and eccentricity resting on an elastic foundation and subjected to an axial load. An exact solution for the free vibrations of a non-uniform beam carrying multiple elastic-supported rigid bars using the numerical assembly method was determined by Lin [31]. Attarnejad et al. [32] proposed the dynamic basic displacement functions for the free transverse vibration analysis of non-prismatic beams. Moreover, they studied the effect of the tip mass on the natural frequencies. Applying the power series method of Frobenius, the exact solutions for the free vibrations and buckling of double-tapered columns with elastic foundation and tip mass were obtained by Firouz-Abadi et al. [33]. Wang [34] analyzed the vibration of a tapered cantilever of constant thickness and linearly tapered width with tip mass utilizing the initial value numerical method. A numerical finite difference scheme for the free vibration of non-uniform cantilever beams carrying both transversely and axially eccentric tip mass was presented by Malaeke and Moeenfard [35]. The linear and nonlinear frequency characteristics of a non-uniform cantilever beam with tip mass using the Galerkin approximation and the method of multiple scales were studied

by Sagar Singh et al. [36]. A new method for the determination of approximate values of natural frequencies of cantilever beams with variable axial parameters with a tip mass and spring was proposed by Nikolić and Šalinić [37]. This technique was based on the replacement of the flexible beam by a rigid multibody system. Torabi et al. [38] presented an exact closed-form solution for the free vibration analysis of conical and tapered beams carrying multiple concentrated masses using the Bessel and Dirac's delta functions. Based on the theory of the continuous-mass transfer matrix method, Huang et al. [39] derived a formulation for determining the exact natural frequencies and associated mode shapes of a nonlinearly tapered beam carrying various concentrated elements in the arbitrary boundary conditions. A Chebyshev spectral method with a null space approach for investigating the boundary-value problem of a non-prismatic Euler–Bernoulli beam with generalized boundary or interface conditions and tip mass was proposed by Hsu et al. [40].

As regards the vibration of inhomogeneous and functionally graded (FG) beams with attached masses, apparently, the first closed-form solutions of the vibrating inhomogeneous beam and bar with a tip mass via the semi-inverse method were derived by Elishakoff and coworkers [41, 42]. Huang and Li [43] presented a new approach for the free vibration of AFG beams with non-uniform cross-section using the Fredholm integral equations. De Rosa et al. [44] calculated the free vibration frequencies of an Euler–Bernoulli beam with exponentially varying cross-sections, in the presence of concentrated tip mass and linear dashpot damper using the symbolic software Mathematica. Through a finite-element approach, the free vibration and stability analysis of AFG tapered Timoshenko beams were investigated by Shahba et al. [45]. These researchers studied the effects of the attached mass on the natural frequencies. Wang and Wang [46] presented an exact vibration solution for an exponentially tapered cantilever beam with tip mass and including a flexible base modeled by a rotational spring. The exact frequency equations of the free vibration of the exponentially AFG beams with various classical boundary conditions were derived by Li et al. [47]. In another work, Li [48] studied the free vibration of axially loaded shear beams carrying elastically restrained lumped-tip masses via asymptotic Timoshenko beam theory. Based on the Kausel theory, stability and vibration analysis of axially loaded shear beam-columns carrying elastically restrained mass were investigated by Zhang et al. [49]. Tang et al. [50] derived the exact frequency equations of the free vibration of the exponentially non-uniform AFG Timoshenko beams with classical end supports. The vibration of a non-uniform carbon nanotube with attached mass via the nonlocal Timoshenko beam theory using the transfer function method incorporating with the perturbation method was investigated by Tang et al. [51]. Yuan et al. [52] proposed an exact analytical approach to solve the free vibrations of axially inhomogeneous Timoshenko beams with variable cross-section and attached point mass. Based on the initial value method, Chen et al. [53] presented a new approach for determining the natural frequencies of AFG nanowires carrying a nanoparticle at the tip via the Timoshenko beam theory incorporating the surface effects. The free vibration analysis of an FG nano-beam with an attached mass at the tip according to Euler–Bernoulli beam theory was analyzed by Rahmani et al. [54]. Using the rigid multibody method, Nikolić [55] studied the free vibration analysis of NAFG cantilever beams with a tip body. Applying the Ritz method, the free vibrations of AFG cantilever tapered beams carrying attached masses were investigated by Rossit et al. [56]. The transverse vibration of a functionally graded material (FGM) cantilever nano-beam carrying a concentrated mass at the free end applying the analytical solution was studied by Ghadiri and Jafari [57]. A new non-iterative computational technique for the free vibration analysis of NAFG rods and beams via the symbolic-numeric method of initial parameters was proposed by Šalinić et al. [58]. Rossit et al. [59] investigated the effect of considering the theory of Timoshenko on the vibration of AFG cantilever beams carrying concentrated masses using the Rayleigh–Ritz method. Based on the Myklestad method which is also known as the transfer matrix method, Mahmoud [60] presented a general solution for the free transverse vibration of NAFG cantilevers loaded at the tips with point masses. The initial value method was applied by Sun and Li [61] to study the free vibration of NAFG Timoshenko beams. The comparison between the forced vibration of isotropic homogeneous and AFG beams carrying concentrated masses was performed by Nguyen et al. [62]. They investigated the influences of the concentrated masses and the varying of the material properties along the simply supported beam on the receptance matrix. Li et al. [63] developed an analytical solution for the free vibration of exponential FG beams with variable cross-sections resting on Pasternak elastic foundations. A Generalized finite-element approach toward the free vibration analysis of NAFG beams was proposed by Sahu et al. [64]. Recently, Liu et al. [65] presented a closed-form dynamic stiffness formulation for the exact transverse free vibration analysis of linearly tapered and/or NAFG beams based on the Euler–Bernoulli theory.

According to the literature review, there is no published work on the exact solutions of the free transverse vibration of the NAFG beams with end point masses and general boundary conditions. Moreover, there is no comprehensive

report on the effects of the attached end point masses on the natural frequencies of the power-law NAFG beams. To overcome these shortages, the analytical approach presented in reference [1] will be extended to obtain the exact natural frequencies of the NAFG Euler–Bernoulli beams with attached end masses and general boundary conditions. In this way, based on the Euler–Bernoulli beam theory, the governing differential equation of motion was solved accurately using the Bessel functions. Then, the constant coefficients matrices of the power-law NAFG beams with the end point masses and general elastic supports were derived by applying the boundary conditions. Accordingly, by taking the constant coefficients matrix determinant equal to zero and calculating the positive real roots, the natural frequencies were obtained. By comparing the responses of the numerical examples with the available solutions, the accuracy, capability, and efficiency of the proposed formulations are demonstrated. Subsequently, the effects of the attached end point masses, rotational and translational elastic supports, and NAFG parameters on the values of the first four natural frequencies of the power-law NAFG beams for the eight parametric cases will be studied comprehensively. It is reminded that the material and geometrical properties of the NAFG beams are assumed to vary continuously and together in the axial length according to the power-law forms. The exact analytical solutions are listed in tabular and graphical forms and can be utilized as the benchmark solutions. Moreover, the results presented herein can be used for the proper design of composite beams carrying end point masses with different elastic boundary conditions.

Free Transverse Vibration Formulation

In this work, the analytical solutions to obtain the exact natural frequencies of the power-law NAFG Euler–Bernoulli beam with attached end point masses and general boundary conditions are presented.

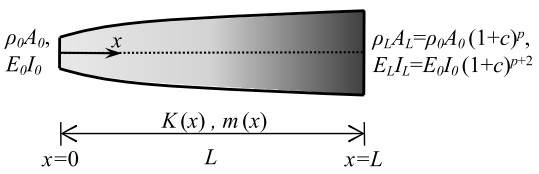

Fig. 1 Schematic of the non-uniform axially functionally graded (NAFG) beam with power-law form

NAFG Material and Geometrical Properties

In the present study, the material and geometrical properties, i.e., mass per unit length and flexural rigidity of the NAFG beam, shown in Fig. 1, are assumed to vary continuously and together in the axial direction according to the power-law forms and defined as:

$$m(x) = \rho(x)A(x) = \rho_0 A_0 \left(1 + c\frac{x}{L}\right)^p = \rho_L A_L \left(\frac{1 + c\frac{x}{L}}{1+c}\right)^p, \tag{1a}$$

$$K(x) = E(x)I(x) = E_0 I_0 \left(1 + c\frac{x}{L}\right)^{p+2} = E_L I_L \left(\frac{1 + c\frac{x}{L}}{1+c}\right)^{p+2}, \tag{1b}$$

where x is the axial coordinate, L is the length of the beam, $m(x) = \rho(x)A(x)$ is the unit mass length of the NAFG beam, which is computed by volume mass density $\rho(x)$ and cross-section area $A(x)$, and $K(x) = E(x)I(x)$ is the flexural rigidity of the NAFG beam which is calculated by the modulus of elasticity $E(x)$ and moment of inertia $I(x)$. Also, ρ_0, A_0, E_0, and I_o are the mass density, cross-section area, modulus of elasticity, and moment of inertia at $x = 0$, respectively. Similarly, ρ_L, A_L, E_L, and I_L are the mass density, cross-section area, modulus of elasticity, and moment of inertia at $x = L$, respectively. Moreover, p and c are the NAFG parameters that p is an integer quantity and represents the gradient index and c represents the gradient coefficient. It should be noted that the mass per unit length and flexural rigidity of the NAFG beam are positive values and therefore $c > -1$. In addition, it is evident that when $c = 0.0$, the beam is uniform, i.e., the material and geometrical properties are kept constant.

It is reminded that changing the mass per unit length $m(x)$ and flexural rigidity $K(x)$ can be expressed based on the variations of the material properties or geometrical properties or both of them. According to this point, the tapered, wedged, stepped, and non-prismatic beams can be considered as the special case of the NAFG beams with constant material and variable geometry [1]. For better understanding, the normalized variations of $m(x)$ and $K(x)$ of the NAFG beam, which are normalized by the values of the material and geometrical properties of the beam at $x = L$, are plotted in Fig. 2 for various values of the gradient index (p) and gradient coefficient (c).

Governing Differential Equation

The free transverse vibration differential equation of a NAFG Euler–Bernoulli beam of length L with end point masses and elastic supports, as shown in Fig. 3, is given by [66]:

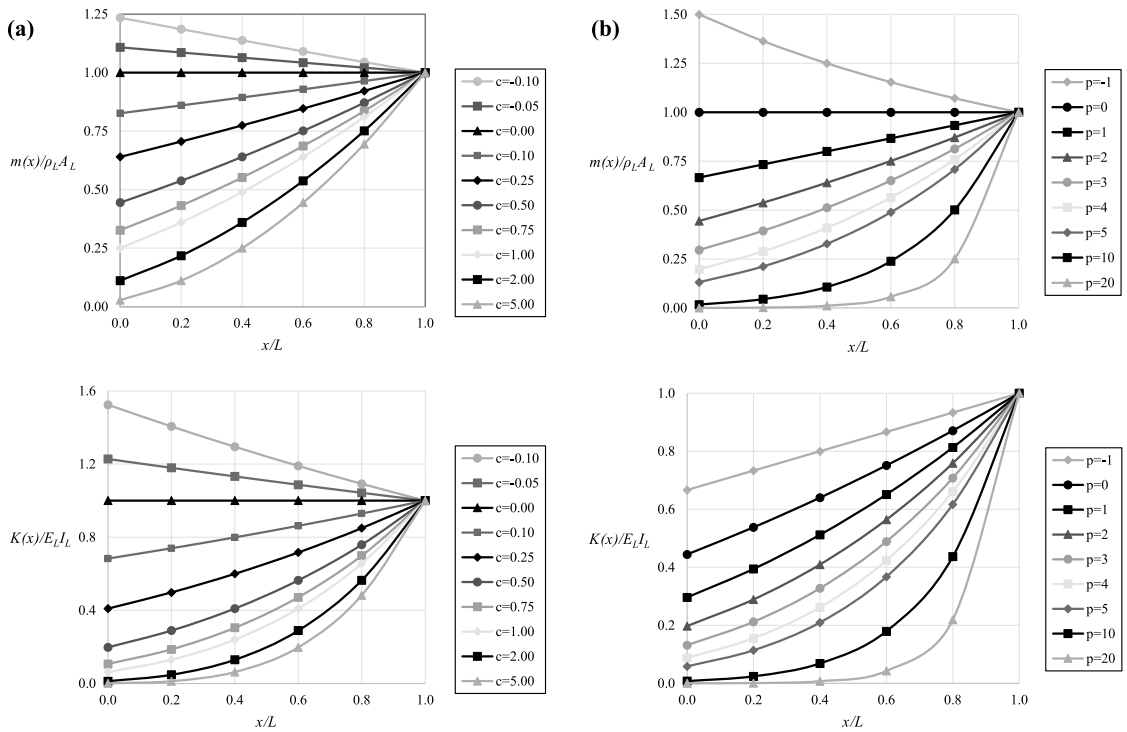

Fig. 2 Normalized variations of mass per unit length and flexural rigidity of the NAFG beam: **a** for various values of gradient index (p) in which $c=0.5$; **b** for various values of gradient coefficient (c) in which $p=2$

$$\frac{\partial^2}{\partial x^2}\left[K(x)\frac{\partial^2 w(x,t)}{\partial x^2}\right]+m(x)\frac{\partial^2 w(x,t)}{\partial t^2}=0,\quad 0<x<L, \tag{2}$$

where x is the axial coordinate, t is time, $w(x,t)$ is the lateral deflection of the beam, $K(x)=E(x)I(x)$ is the flexural rigidity of the beam at the position x and $m(x)=\rho(x)A(x)$ is the mass per unit length of the beam at the position x.

Following the separation of variable analogy, the solution of Eq. (2) can be expressed as [66]:

$$w_i(x,t)=W_i(x)e^{j\omega_i t}\quad (j^2=-1), \tag{3}$$

where ω_i is the circular frequency and $W_i(x)$ is the shape function of the lateral motion of the ith vibration mode.

Substituting the Eq. (3) into Eq. (2), one can get:

$$\frac{d^2}{dx^2}\left[K(x)\frac{d^2 W_i(x)}{dx^2}\right]-m(x)\omega_i^2 W_i(x)=0. \tag{4}$$

If Eqs. (1a) and (1b) are inserted into Eq. (4), it can be rewritten as:

$$\begin{aligned}&\left(1+c\frac{x}{L}\right)^{p+2}\frac{d^4 W_i(x)}{dx^4}+2\frac{c}{L}(p+2)\left(1+c\frac{x}{L}\right)^{p+1}\frac{d^3 W_i(x)}{dx^3}\\&+\frac{c^2}{L^2}(p+1)(p+2)\left(1+c\frac{x}{L}\right)^{p}\frac{d^2 W_i(x)}{dx^2}-\frac{\rho_0 A_0\omega_i^2}{E_0 I_0}\left(1+c\frac{x}{L}\right)^{p}W_i(x)=0.\end{aligned} \tag{5}$$

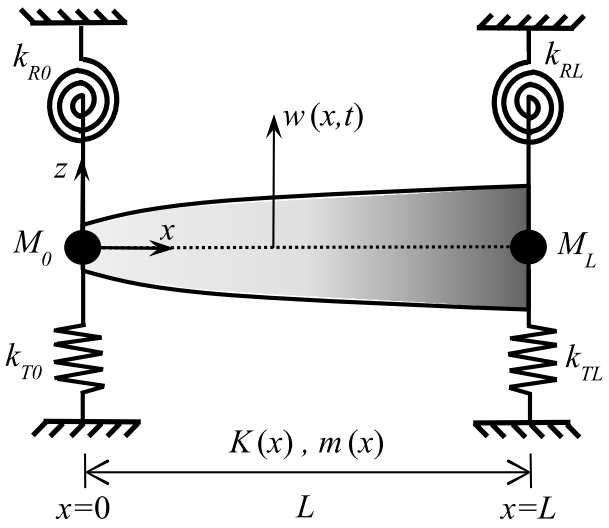

Fig. 3 Schematic of the NAFG beam with end point masses and elastic supports

Introducing the following quantity

$$X = \left(1 + c\frac{x}{L}\right), \tag{6}$$

which is equal to 1 at $x=0$ and to $1+c$ at $x=L$, and considering in mind that

$$\mathrm{d}x = \left(\frac{L}{c}\right)\mathrm{d}X. \tag{7}$$

Equation (5) simplifies as follows:

$$X^{p+2}\frac{d^4W_i(X)}{\mathrm{d}X^4} + 2(p+2)X^{p+1}\frac{d^3W_i(X)}{\mathrm{d}X^3} + (p+1)(p+2)X^p\frac{d^2W_i(X)}{\mathrm{d}X^2} - \frac{\Omega_i^4}{c^4}X^pW_i(X) = 0, \tag{8}$$

where $\Omega_i = \sqrt[4]{\frac{\rho_0 A_0 \omega_i^2 L^4}{E_0 I_0}}$ is the dimensionless natural frequency coefficient of the ith vibration mode.

The general solution of this equation for the positive gradient coefficient (i.e., $c>0$) is [67, 68]:

$$W_i(X) = X^{-\frac{p}{2}}\left[C_1J_p\left(\frac{2\Omega_i\sqrt{X}}{c}\right) + C_2Y_p\left(\frac{2\Omega_i\sqrt{X}}{c}\right) + C_3I_p\left(\frac{2\Omega_i\sqrt{X}}{c}\right) + C_4K_p\left(\frac{2\Omega_i\sqrt{X}}{c}\right)\right], \tag{9}$$

where C_1, C_2, C_3, C_4 are unknown constants and J_p, Y_p, I_p, K_p are, respectively, the Bessel functions of first, second, modified first, and modified second kinds of order p. The detail of the derivation of the general solution Eq. (9) is presented in Appendix A.

It is reminded that the general solution of Eq. (8) for $c=0$ (i.e., uniform and isotropic homogenous beam) and negative gradient coefficients (i.e., $-1<c<0$) are expressed with Eqs. (10) and (11), respectively [68].

$$W_i(X) = C_1\sin(X) + C_2\cos(X) + C_3\sinh(X) + C_4\cosh(X), \tag{10}$$

$$W_i(X) = X^{-\frac{p}{2}}\left[C_1J_p\left(-\frac{2\Omega_i\sqrt{X}}{c}\right) + C_2Y_p\left(-\frac{2\Omega_i\sqrt{X}}{c}\right) + C_3I_p\left(-\frac{2\Omega_i\sqrt{X}}{c}\right) + C_4K_p\left(-\frac{2\Omega_i\sqrt{X}}{c}\right)\right]. \tag{11}$$

General Boundary Conditions

The boundary conditions, in the presence of end point masses M_0, M_L and constraints with the rotational elastic stiffnesses k_{R0}, k_{RL} and lateral translational elastic stiffnesses k_{T0}, k_{TL} are expressed as [66]:

$$K(x)\frac{d^2W_i(x)}{\mathrm{d}x^2} - k_{R0}\frac{\mathrm{d}W_i(x)}{\mathrm{d}x} = 0, \tag{12}$$

$$\frac{d}{\mathrm{d}x}\left[K(x)\frac{d^2W_i(x)}{\mathrm{d}x^2}\right] + k_{T0}W_i(x) - M_0\omega_i^2W_i(x) = 0, \tag{13}$$

which refer to the equilibrium of the bending moment and shear force at $x=0$, respectively, and

$$K(x)\frac{d^2W_i(x)}{\mathrm{d}x^2} + k_{RL}\frac{\mathrm{d}W_i(x)}{\mathrm{d}x} = 0, \tag{14}$$

$$\frac{d}{\mathrm{d}x}\left[K(x)\frac{d^2W_i(x)}{\mathrm{d}x^2}\right] - k_{TL}W_i(x) + M_L\omega_i^2W_i(x) = 0, \tag{15}$$

which denote to the equilibrium of the bending moment and shear force at $x=L$, respectively.

Substituting Eq. (1b) and utilizing Eqs. (6) and (7), the boundary conditions become:

$$X^{p+2}\frac{d^2W_i(X)}{\mathrm{d}X^2} - \frac{k_{R0}L}{E_0I_0c}\frac{\mathrm{d}W_i(X)}{\mathrm{d}X} = 0, \tag{16}$$

$$X^{p+2}\frac{d^3W_i(X)}{\mathrm{d}X^3} + (p+2)X^{p+1}\frac{d^2W_i(X)}{\mathrm{d}X^2} + \frac{(k_{T0}-M_0\omega_i^2)L^3}{E_0I_0c^3}W_i(X) = 0, \tag{17}$$

at $X=1$ ($x=0$), and

$$X^{p+2}\frac{d^2W_i(X)}{\mathrm{d}X^2} + \frac{k_{RL}L}{E_0I_0c}\frac{\mathrm{d}W_i(X)}{\mathrm{d}X} = 0, \tag{18}$$

$$X^{p+2}\frac{d^3W_i(X)}{\mathrm{d}X^3} + (p+2)X^{p+1}\frac{d^2W_i(X)}{\mathrm{d}X^2} + \frac{(M_L\omega_i^2-k_{TL})L^3}{E_0I_0c^3}W_i(X) = 0, \tag{19}$$

at $X=1+c$ ($x=L$).

For simplicity, the following dimensionless mass ratios (α_0, α_L) and stiffness ratios (R_0, R_L, T_0 and T_L) are introduced:

$$\alpha_0 = \left.\frac{M_0}{\rho_0A_0LX^2}\right|_{X=1} = \frac{M_0}{\rho_0A_0L}, R_0 = \frac{k_{R0}L}{E_0I_0}, T_0 = \frac{k_{T0}L^3}{E_0I_0}$$
$$\alpha_L = \left.\frac{M_L}{\rho_LA_LLX^2}\right|_{X=1+c} = \frac{M_L}{\rho_LA_LL(1+c)^2}, R_L = \frac{k_{RL}L}{E_LI_L}, T_L = \frac{k_{TL}L^3}{E_LI_L}. \tag{20}$$

By replacing the X values and considering the dimensionless natural frequency coefficient, Ω_i and dimensionless ratios defined as Eq. (20), the boundary conditions of Eqs. (16)–(19) can be expressed by the following non-dimensional forms:

$$W_i''(1) - \frac{R_0}{c} W_i'(1) = 0, \tag{21}$$

$$W_i'''(1) + (p+2) W_i''(1) + \frac{(T_0 - \alpha_0 \Omega_i^4)}{c^3} W_i(1) = 0, \tag{22}$$

$$W_i''(1+c) + \frac{R_L}{c} W_i'(1+c) = 0, \tag{23}$$

$$W_i'''(1+c) + \frac{(p+2)}{(1+c)} W_i''(1+c) + \frac{(\alpha_L \Omega_i^4 - T_L)}{c^3} W_i(1+c) = 0, \tag{24}$$

where $W_i'(X) = \frac{dW_i(X)}{dX}$, $W_i''(X) = \frac{d^2 W_i(X)}{d^2 X}$, $W_i'''(X) = \frac{d^3 W_i(X)}{d^3 X}$.

Determination of the Natural Frequency

By substituting the general solution (9) into the non-dimensional boundary conditions given in Eqs. (21)–(24), a homogeneous system of four equations for the four integration constants (i.e., C_1, C_2, C_3, C_4) can be obtained as:

$$\begin{bmatrix} A_{11} & A_{12} & A_{13} & A_{14} \\ A_{21} & A_{22} & A_{23} & A_{24} \\ A_{31} & A_{32} & A_{33} & A_{34} \\ A_{41} & A_{42} & A_{43} & A_{44} \end{bmatrix} \begin{bmatrix} C_1 \\ C_2 \\ C_3 \\ C_4 \end{bmatrix} = \begin{bmatrix} 0 \\ 0 \\ 0 \\ 0 \end{bmatrix}, \tag{25}$$

or in compact matrix form as follows:

$$\mathrm{AC} = 0, \tag{26}$$

where the constant coefficients matrix **A** for the NAFG beams with the various gradient coefficient are given explicitly in Appendix B. To have a non-trivial solution, the determinant of this system must be zero:

$$\det \mathrm{A} = 0. \tag{27}$$

Consequently, having the values of p, c, α_0, α_L, T_0, T_L, R_0, and R_L, positive real roots of this equation are the natural frequency coefficients Ω_i of the NAFG beams with the end point masses and elastic end supports, shown in Fig. 3. It should be added, these were calculated numerically.

Numerical Examples and Verification

To confirm the accuracy, application, and efficiency of the derived formulations, five numerical examples, shown in Fig. 4a–e, are analyzed in this part. The results are compared with those obtained by other researchers. It should be noted, using the proposed formulations, one can find the exact natural frequencies of the NAFG beams with attached masses and general boundary conditions at both ends. Accordingly, if the stiffness ratios are allowed to become infinity

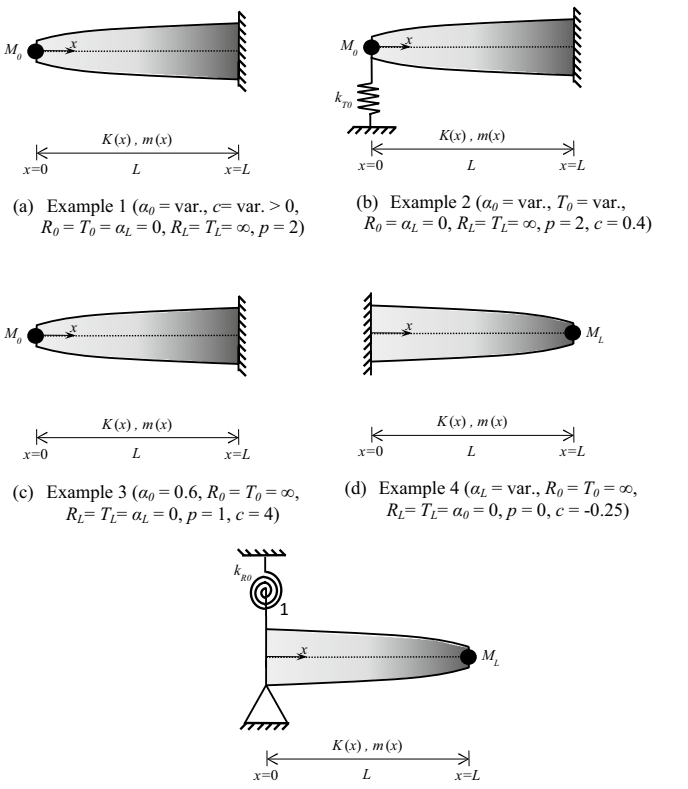

(a) Example 1 (α_0 = var., c= var. > 0, $R_0 = T_0 = \alpha_L = 0$, $R_L = T_L = \infty$, $p = 2$)

(b) Example 2 (α_0 = var., T_0 = var., $R_0 = \alpha_L = 0$, $R_L = T_L = \infty$, $p = 2$, $c = 0.4$)

(c) Example 3 ($\alpha_0 = 0.6$, $R_0 = T_0 = \infty$, $R_L = T_L = \alpha_L = 0$, $p = 1$, $c = 4$)

(d) Example 4 (α_L = var., $R_0 = T_0 = \infty$, $R_L = T_L = \alpha_0 = 0$, $p = 0$, $c = -0.25$)

(e) Example 5 (α_L = var., c = var. < 0, R_0 = var., $T_0 = \infty$, $R_L = T_L = \alpha_0 = 0$, $p = 1$)

Fig. 4 Schematic of the NAFG beams with end point masses and different boundary conditions in numerical examples

Table 1 First five dimensionless natural frequency coefficients Ω_i, $i=1,2,3,4,5$ of the NAFG beam ($p=2$, $c=\text{var.}>0$) for $T_0=R_0=\alpha_L=0$, $T_L=R_L=\infty$ and various values of α_0 in Example 1

c	α_0	Ω_i	Present	Hsu et al. [40]	Attarnejad et al. [32]	Lai et al. [30]	Auciello [17]	Mabie and Rogers [3]
0.2	0.242667	$i=1$	1.805113	1.805113	–	1.805116	1.805113	1.805112
		$i=2$	4.531399	4.531398	–	4.531398	4.531399	4.531402
		$i=3$	7.682832	7.682832	–	7.682833	7.682832	7.682832
		$i=4$	10.901161	–	–	–	–	10.901147
		$i=5$	14.149914	–	–	–	–	14.149912
	0.728000	$i=1$	1.519988	–	–	1.519992	1.519988	1.519987
		$i=2$	4.343868	–	–	4.343868	4.343868	4.343869
		$i=3$	7.542352	–	–	7.542352	7.542352	7.542354
		$i=4$	10.793331	–	–	–	–	10.793331
		$i=5$	14.062817	–	–	–	–	14.062823
	1.213333	$i=1$	1.373712	–	–	1.373710	1.373712	1.373710
		$i=2$	4.289384	–	–	4.289385	4.289384	4.289382
		$i=3$	7.507077	–	–	7.507076	7.507077	7.507077
		$i=4$	10.768049	–	–	–	–	10.768055
		$i=5$	14.043144	–	–	–	–	14.043148
	2.426667	$i=1$	1.180607	1.180606	–	1.180605	1.180607	1.180606
		$i=2$	4.242896	4.242896	–	4.242897	4.242896	4.242900
		$i=3$	7.478641	7.478641	–	7.478641	7.478642	7.478643
		$i=4$	10.748142	–	–	–	–	10.748163
		$i=5$	14.027839	–	–	–	–	14.027829
1.0	0.200000	$i=1$	2.672324	–	2.6723	–	–	–
		$i=2$	5.606998	–	5.6070	–	–	–
		$i=3$	9.081881	–	9.0819	–	–	–
		$i=4$	12.720860	–	12.7209	–	–	–
		$i=5$	16.425475	–	–	–	–	–
	0.466667	$i=1$	2.392505	2.392504	–	2.392498	2.392505	2.392505
		$i=2$	5.375542	5.375541	–	5.375538	5.375542	5.375537
		$i=3$	8.914098	8.914098	–	8.914100	8.914098	8.914101
		$i=4$	12.595271	–	–	–	–	12.595277
		$i=5$	16.325968	–	–	–	–	16.325961
	0.500000	$i=1$	2.366312	–	2.3663	–	–	–
		$i=2$	5.359812	–	5.3598	–	–	–
		$i=3$	8.904012	–	8.9040	–	–	–
		$i=4$	12.588136	–	12.5881	–	–	–
		$i=5$	16.320485	–	–	–	–	–
	1.000000	$i=1$	2.088116	–	2.0881	–	–	–
		$i=2$	5.233157	–	5.2331	–	–	–
		$i=3$	8.827802	–	8.8278	–	–	–
		$i=4$	12.535573	–	12.5356	–	–	–
		$i=5$	16.280604	–	–	–	–	–
	1.400000	$i=1$	1.949585	–	–	1.949576	1.949585	1.949585
		$i=2$	5.190740	–	–	5.190742	5.190740	5.190742
		$i=3$	8.804081	–	–	8.804084	8.804081	8.804079
		$i=4$	12.519671	–	–	–	–	12.519665
		$i=5$	16.268711	–	–	–	–	16.268712
	2.000000	$i=1$	1.805129	–	1.8051	–	–	–
		$i=2$	5.156789	–	5.1568	–	–	–
		$i=3$	8.785676	–	8.7857	–	–	–

Table 1 (continued)

c	α_0	Ω_i	Present	Hsu et al. [40]	Attarnejad et al. [32]	Lai et al. [30]	Auciello [17]	Mabie and Rogers [3]
		$i=4$	12.507474	–	12.5075	–	–	–
		$i=5$	16.259640	–	–	–	–	–
	2.333333	$i=1$	1.744161	–	–	1.744152	1.744161	1.744162
		$i=2$	5.145038	–	–	5.145041	5.145038	5.145036
		$i=3$	8.779421	–	–	8.779423	8.779421	8.779419
		$i=4$	12.503355	–	–	–	–	12.503360
		$i=5$	16.256587	–	–	–	–	16.256599
	4.666667	$i=1$	1.485718	1.485717	–	1.485704	1.485718	1.485715
		$i=2$	5.108412	5.108411	–	5.108415	5.108412	5.108415
		$i=3$	8.760283	8.760282	–	8.760286	8.760283	8.760285
		$i=4$	12.490840	–	–	–	–	12.490837
		$i=5$	16.247341	–	–	–	–	16.247338

or zero, then the classical restraints can be easily recovered. For example, if $R_0=T_0=\infty$ and $R_L=T_L=0$, then the beam is considered as the cantilevered beam. If $R_0=R_L=0$ and $T_0=T_L=\infty$, then the frequency equation of the simply supported beam is obtained. If $R_0=R_L=\infty$ and $T_0=T_L=\infty$, then the beam is considered as the clamped–clamped beam.

Example 1. In this sample, the first five dimensionless natural frequency coefficients Ω_i, $i=1,2,3,4,5$ for the NAFG beam ($p=2$, $c=\text{var.}>0$) with $T_0=R_0=\alpha_L=0$, $T_L=R_L=\infty$ and various values of α_0 and c (i.e., Fig. 4a) are calculated and arranged in Table 1. Table 1 shows the results of the present study, as well as those other methods. Based on the data shown in Table 1, it is observed that the proposed formulation for computing the natural frequencies has high accuracy and efficiency.

Example 2. In this example, the first four dimensionless natural frequency coefficients Ω_i, $i=1,2,3,4$ of the NAFG beam ($p=2$, $c=0.4$) for $R_0=\alpha_L=0$, $T_L=R_L=\infty$ and various values of T_0 and α_0 (i.e., Fig. 4b) are computed and presented in Table 2. From Table 2, it is concluded that results of the present method are very close to the values obtained by other techniques.

Example 3. In this sample, the first five natural frequencies ω_i, $i=1,2,3,4,5$ are obtained for the NAFG beam ($p=1$, $c=4$) with $T_0=R_0=\infty$, $T_L=R_L=\alpha_L=0$ and $\alpha_0=0.6$ (i.e., Fig. 4c). It should be noted that the numerical values of the mechanical and geometrical properties of the NAFG beam considered as follows: $L=1.6$ m, $A_0=b_0\times h_0=0.1\times 0.08$, $I_0=b_0\times h_0^3/12=0.1\times 0.08^3/12$, $M_0=60.288$ kg, $\rho_0=7850$ kg/m^3, $E_0=2.051\times 10^{11}$ N/m^2, $\alpha_0=60.288/(7850\times 0.1\times 0.08\times 1.6)=0.6$, $\rho_0 A_0=7850\times 9.81\times 0.1\times 0.08=616.068$ N/m, and $E_0I_0=2.051\times 10^{11}\times 0.1\times 0.08^3/12=875{,}093.333\,3$ N m^2 [25]. A comparison of the results with the other approaches is listed in Table 3. According to the findings, the prediction of the proposed technique agree well with those other approaches.

Example 4. In this example, the first square six dimensionless natural frequency coefficients Ω_i^2, $i=1,2,3,4,5,6$ of the NAFG beam ($p=0$, $c=-0.25$) for $T_0=R_0=\infty$, $T_L=R_L=\alpha_0=0$ and various values of α_L (i.e., Fig. 4d) are obtained and arranged in Table 4. Table 4 shows the results of the present method, as well as the recent work of Mahmoud [60].

Example 5. In this sample, the first square three dimensionless natural frequency coefficients Ω_i^2, $i=1,2,3$ are calculated for the NAFG beam ($p=1$, $c=\text{var.}<0$) with $T_0=\infty$, $T_L=R_L=\alpha_0=0$ and various values of R_0, α_L, and c (i.e., Fig. 4(e)). A comparison of the results with those computed by [34] is listed in Table 5. According to the results, the proposed approach gives a high accuracy prediction. Note that, in Table 5, the results from Çelik [69] are given in square brackets.

Parametric Studies and Discussion

In this section, eight parametric cases, as shown in Fig. 5a–h, with the classical and non-classical boundary conditions will be considered and the effects of the attached end masses, elastic supports, and NAFG parameters on the first four natural frequencies of them will be investigated comprehensively. It should be noted that the NAFG parameters in all cases, except case 8, are considered identical to compare the results of one case with other cases. In other words, in these cases, the dynamic behavior of the NAFG beams with $p=2$ and $c=0.5$ are studied.

Table 2 First four dimensionless natural frequency coefficients Ω_i, $i=1,2,3,4$ of the NAFG beam ($p=2$, $c=0.4$) for $R_0=\alpha_L=0$, $T_L=R_L=\infty$ and various values of T_0 and α_0 in Example 2

T_0	α_0	Ω_i	Present	Çelik [69]	Nikolić and Šalinić [37]	Mao [70]	Hsu et al.[71]	De Rosa and Auciello [72]
0	0	$i=1$	2.376612	2.376612	2.37658	–	2.37661	2.3766
		$i=2$	5.373870	5.373870	5.37363	–	5.37387	5.3739
		$i=3$	8.726374	8.726374	8.72538	–	8.72637	8.7264
		$i=4$	12.113521	12.113521	12.1108	–	12.11351	12.1135
	1	$i=1$	1.602596	–	1.60258	–	–	–
		$i=2$	4.562011	–	4.56185	–	–	–
		$i=3$	7.875659	–	7.87485	–	–	–
		$i=4$	11.257316	–	11.2549	–	–	–
	10	$i=1$	0.946758	–	0.94675	–	–	–
		$i=2$	4.447496	–	4.44734	–	–	–
		$i=3$	7.808817	–	7.80801	–	–	–
		$i=4$	11.211446	–	11.2091	–	–	–
1	0	$i=1$	2.442011	2.442011	2.44198	2.44004	2.44201	2.4420
		$i=2$	5.380548	5.380548	5.38031	5.37513	5.38055	5.3805
		$i=3$	8.727984	8.727984	8.72699	8.71912	8.72798	8.7280
		$i=4$	12.114128	12.114129	12.11141	12.10182	12.11412	12.1141
	1	$i=1$	1.649095	–	1.64908	–	–	–
		$i=2$	4.562271	–	4.56211	–	–	–
		$i=3$	7.875677	–	7.80380	–	–	–
		$i=4$	11.257319	–	11.2549	–	–	–
	10	$i=1$	0.974286	–	0.97428	–	–	–
		$i=2$	4.447499	–	4.44734	–	–	–
		$i=3$	7.808817	–	7.80801	–	–	–
		$i=4$	11.211446	–	11.2091	–	–	–
1000	0	$i=1$	4.375503	4.375503	4.37536	4.37154	4.37550	4.3755
		$i=2$	7.477211	7.477211	7.47657	7.47233	7.47721	7.4772
		$i=3$	10.221535	10.221535	10.2202	10.21795	10.22153	10.2215
		$i=4$	12.857197	12.857197	12.8545	12.85023	12.85719	12.8572
	1	$i=1$	4.343813	–	4.34368	–	–	–
		$i=2$	5.580504	–	5.58046	–	–	–
		$i=3$	7.899077	–	7.89828	–	–	–
		$i=4$	11.260539	–	11.2582	–	–	–
	10	$i=1$	3.146022	–	3.14602	–	–	–
		$i=2$	4.452386	–	4.45223	–	–	–
		$i=3$	7.809036	–	7.80823	–	–	–
		$i=4$	11.211480	–	11.2091	–	–	–

Table 3 First five natural frequencies ω_i, $i=1,2,3,4,5$ of the NAFG beam ($p=1$, $c=4$) for $T_0=R_0=\infty$, $T_L=R_L=\alpha_L=0$ and $\alpha_0=0.6$ in Example 3

ω_i	Present	Rossit et al. [56]	Chen and Liu [29]	Wu and Chen [25]	FEM [25]
$i=1$	569.37469	569.3747	569.6279	569.6273	569.3039
$i=2$	2503.71434	2503.714	2508.895	2508.8947	2503.2976
$i=3$	6710.26762	6710.268	6743.232	6743.2318	6709.0487
$i=4$	13,288.99814	13,289.00	13,408.53	13,408.5313	13,286.4974
$i=5$	22,240.74451	22,240.74	22,570.17	22,570.1693	22,236.4917

Table 4 First square six dimensionless natural frequency coefficients Ω_i^2, $i=1,2,3,4,5,6$ of the NAFG beam ($p=0$, $c=-0.25$) for $T_0=R_0=\infty$, $T_L=R_L=\alpha_0=0$ and various values of α_L in Example 4

Ω_i^2	$\alpha_L=0.0$		$\alpha_L=0.3$		$\alpha_L=0.6$		$\alpha_L=0.9$	
	Present	Mahmoud [60]	Present	Mahmoud [60]	Present	Mahmoud [60]	Present	Mahmoud [60]
$i=1$	3.33677	3.337	2.22025	2.220	1.77570	1.776	1.52200	–
$i=2$	19.71504	19.715	15.59269	15.593	14.81344	14.813	14.48662	–
$i=3$	54.23107	54.232	46.01331	46.013	45.00780	45.008	44.62107	–
$i=4$	105.77354	105.775	93.39024	93.390	92.29161	92.292	91.88649	–
$i=5$	174.50883	174.512	157.89870	157.899	156.74554	156.746	156.33008	–
$i=6$	260.42601	260.431	239.56432	239.565	238.37610	238.376	237.95424	–

Effects of the End Mass with Different Elastic Boundary Conditions (Case 1 up to Case 6)

In Figs. 6 through 11, the effects of the end mass ratios (i.e., α_0 and α_L) with the various rotational and translational stiffness ratios (i.e., R_0, T_0, R_L, and T_L), on the first four dimensionless natural frequency coefficients Ω_i ($i=1,2,3,4$) for the NAFG beams ($p=2$, $c=0.5$) introduced as case 1 up to case 6 are investigated, respectively. Moreover, the corresponding numerical values of Ω_i ($i=1,2,3,4$) for these cases are tabulated in Tables 6 through 11, respectively.

Case 1

Based on data shown in Table 6, it is concluded that for the free supported NAFG beam with the translational spring at $x=0$, rotational spring at $x=L$, and attached point mass at $x=0$ (Fig. 5a), as the end mass ratio α_0 increases from 0.0 up to 1.0, the first four dimensionless natural frequency coefficients of the NAFG beam decrease from 0.4930, 1.4212, 5.3358 and 8.7880, and tend to 0.4407, 1.1083, 4.4127 and 7.8922 for the low stiffness ratios ($T_0=R_L=0.1$), respectively. Also, for the moderate stiffness ratios ($T_0=R_L=10$) in case 1, increasing α_0 from 0.0 to 1.0, causes reduce in the values of Ω_i ($i=1,2,3,4$) of the NAFG beam from 1.4040, 3.1853, 6.1207 and 9.4310, and approach 1.3233, 2.2333, 5.2170 and 8.5506, respectively. Furthermore, when the end mass ratio α_0 in this case changes, the first four dimensionless natural frequency coefficients of the NAFG beam remain almost constant for the high stiffness ratios ($T_0=R_L=10^5$). In other words, this latter state corresponds to a pinned-guided beam, and evidently, the effect of α_0 on the natural frequencies of the beam is very insignificant.

According to Fig. 6 and Table 6, it is observed that increasing the end mass ratio α_0 always causes a decrease in the values of Ω_i ($i=1,2,3,4$) for the beam, regardless of the quantities of the stiffness ratios. On average and based on the amounts of Ω_i ($i=1,2,3,4$), Ω_1 and Ω_2, in this case, have the lowest and highest sensitivity to the variation of the end mass ratio, respectively. Accordingly, the second dimensionless natural frequency coefficient in case 1 can reduce by nearly 31% whenever the end mass ratio α_0 increases from 0.0 to 1.0 for $T_0=R_L=50$. On the other hand, by increasing the stiffness ratios, Ω_i ($i=1,2,3,4$) of the beam always increases, irrespective of the amount of the end mass ratio. At the most sensitive state, increasing T_0 and R_L from the low stiffness ratios ($T_0=R_L=0.1$) to the high stiffness ratios ($T_0=R_L=10^5$) for $\alpha_0=1.0$, can raise the quantity of Ω_2 for the NAFG beam in case 1 by about 4.8 times.

Case 2

By observing data in Table 7, it is founded that for the free-pinned supported NAFG beam with the translational spring at $x=0$, rotational spring at $x=L$, and attached point mass at $x=0$ (Fig. 5b), when the end mass ratio α_0 increases from 0.0 up to 1.0, the first four dimensionless natural frequency coefficients of the NAFG beam decrease from 1.0869, 4.5849, 7.9935 and 11.4515, and tend to 0.8009, 3.7027, 7.1045 and 10.5630 for the low stiffness ratios ($T_0=R_L=0.1$), respectively. In addition, for the moderate stiffness ratios ($T_0=R_L=10$) in case 2, increasing α_0 from 0.0 to 1.0, causes reduce in the values of Ω_i ($i=1,2,3,4$) of the NAFG beam from 2.7866, 5.2765, 8.4984 and 11.8510, and approach 1.9490, 4.3986, 7.6248 and 10.9774, respectively. Besides, as the end mass ratio α_0 in this case varies, the first four dimensionless natural frequency coefficients of the NAFG beam stay almost constant for the high stiffness ratios ($T_0=R_L=10^5$). In other words, this latter state corresponds to a pinned-fixed beam, and clearly, the effect of α_0 on the natural frequencies of the beam is very negligible.

As seen in Fig. 7 and Table 7, it is concluded that increasing the end mass ratio α_0 always causes a decrease in the values of Ω_i ($i=1,2,3,4$) for the beam, regardless of the quantities of the stiffness ratios. On the average and about the quantities of Ω_i ($i=1,2,3,4$), changing of the end mass ratio α_0 has the minimum and maximum influences on the values of Ω_1 and Ω_4 for this case, respectively. However, the

Table 5 First square three dimensionless natural frequency coefficients Ω_i^2, $i=1,2,3$ of the NAFG beam ($p=1$, $c=\text{var.}<0$) for $T_0=\infty$, $T_L=R_L=\alpha_0=0$ and various values of R_0 and α_L in Example 5

R_0	α_L	Ω_i^2	$c=$-0.1		$c=-0.5$		$c=-0.9$	
			Present	Wang [34]	Present	Wang [34]	Present	Wang [34]
∞	0	$i=1$	3.55870	3.5587 [3.55870207]*	3.82378	3.8238 [3.82378485]	4.63072	4.6307 [4.63072386]
		$i=2$	21.33810	21.338 [21.33810280]	18.31726	18.317 [18.31726090]	14.93079	14.931 [14.93079267]
		$i=3$	58.97990	58.980 [58.97990492]	47.26483	47.265 [47.26482701]	32.83312	32.833 [32.83312116]
	0.1	$i=1$	2.95914	2.9591	2.87371	2.8737	2.38642	2.3864
		$i=2$	18.53302	18.533	14.77618	14.276	9.34342	9.3434
		$i=3$	52.65987	52.660	40.29865	40.299	24.68746	24.688
	1	$i=1$	1.51206	1.5121	1.28035	1.2804	0.84354	0.8435
		$i=2$	15.58661	15.587	12.68104	12.681	8.70534	8.7053
		$i=3$	48.44057	48.441	37.88666	37.887	24.25395	24.254
	10	$i=1$	0.52117	0.5212	0.42577	0.42583	0.26996	0.2700
		$i=2$	14.93063	14.931	12.34024	12.340	8.63768	8.6377
		$i=3$	47.72224	47.722	37.56434	37.564	24.20918	24.209
10	0	$i=1$	3.02797	3.0280	3.36492	3.3649	4.21310	4.2131
		$i=2$	18.78468	18.785	16.31791	16.318	13.64154	13.642
		$i=3$	53.11947	53.120	42.81306	42.813	30.23683	30.237
	0.1	$i=1$	2.54742	2.5474	2.57707	2.5771	2.27330	2.2733
		$i=2$	16.35841	16.358	13.18767	13.188	8.46985	8.4699
		$i=3$	47.43342	47.433	36.45097	36.451	22.55855	22.559
	1	$i=1$	1.32822	1.3282	1.17130	1.1713	0.81309	0.8131
		$i=2$	13.65946	13.660	11.20748	11.208	7.82342	7.8234
		$i=3$	43.44577	43.446	34.12567	34.126	22.12343	22.123
	10	$i=1$	0.46073	0.4607	0.39118	0.3912	0.26057	0.2606
		$i=2$	13.03521	13.035	10.87598	10.876	7.75471	7.7547
		$i=3$	42.75093	42.751	33.81038	33.810	22.07845	22.078
1	0	$i=1$	1.61110	1.6111	1.91091	1.9109	2.57413	2.5741
		$i=2$	15.70035	15.700	13.39463	13.395	11.21081	11.211
		$i=3$	48.57439	48.574	38.70756	38.708	27.10063	27.101
	0.1	$i=1$	1.38703	1.3870	1.53445	1.5345	1.64628	1.6463
		$i=2$	13.56419	13.564	10.60685	10.607	6.29985	6.2999
		$i=3$	43.16171	43.162	32.61051	32.611	19.53331	19.533
	1	$i=1$	0.75783	0.7578	0.74319	0.7432	0.63348	0.6335
		$i=2$	10.97299	10.973	8.58613	8.5861	5.44745	5.4475
		$i=3$	39.19922	39.199	30.24469	30.245	19.05595	19.056
	10	$i=1$	0.26741	0.2674	0.25225	0.2523	0.20495	0.2050
		$i=2$	10.32671	10.327	8.21759	8.2176	5.35256	5.3526
		$i=3$	38.49242	38.492	29.91758	29.918	19.00641	19.006
0.1	0	$i=1$	0.56256	0.5626	0.68230	0.6823	0.94296	0.9430
		$i=2$	14.94902	14.949	12.59742	12.597	10.45590	10.456
		$i=3$	47.74425	47.744	37.89854	37.899	26.40148	26.402
	0.1	$i=1$	0.48829	0.4883	0.55917	0.5592	0.66894	0.6689
		$i=2$	12.85211	12.852	9.83850	9.8385	5.41069	5.4107
		$i=3$	42.35969	42.360	31.81768	31.818	18.77666	18.777
	1	$i=1$	0.27201	0.2720	0.28080	0.2808	0.28346	0.2835
		$i=2$	10.23259	10.333	7.71173	7.7117	4.25931	4.2593
		$i=3$	38.38258	38.383	29.42437	29.424	18.27911	18.279

Table 5 (continued)

R_0	α_L	Ω_i^2	$c=$-0.1		$c=-0.5$		$c=-0.9$	
			Present	Wang [34]	Present	Wang [34]	Present	Wang [34]
	10	$i=1$	0.09678	0.09678	0.09641	0.09641	0.09335	0.09335
		$i=2$	9.55759	9.5576	7.30117	7.3012	4.11277	4.1128
		$i=3$	37.66941	37.669	29.09170	29.092	18.22739	18.227

*The values that are shown in square brackets are given by Çelik [69]

second dimensionless natural frequency coefficient in case 2 can reduce by about 31% whenever the end mass ratio α_0 increases from 0.0 to 1.0 for $T_0=R_L=500$. On the other hand, by increasing the stiffness ratios, Ω_i ($i=1,2,3,4$) of the beam always increases, irrespective of the value of the end mass ratio. At the most sensitive state, increasing T_0 and R_L from the low stiffness ratios ($T_0=R_L=0.1$) to the high stiffness ratios ($T_0=R_L=10^5$) for $\alpha_0=1.0$, can raise the quantity of Ω_1 for the NAFG beam in case 2 by nearly 5.7 times.

Case 3

From data reported in Table 8, it is observed that for the free supported NAFG beam with two translational springs at $x=0$ and $x=L$, and attached point mass at $x=0$ (Fig. 5c), as the end mass ratio α_0 increases from 0.0 up to 1.0, the first four dimensionless natural frequency coefficients of the NAFG beam decrease from 0.6808, 1.0411, 5.3058 and 8.7703, and tend to 0.5137, 0.9657, 4.3737 and 7.8723 for the low stiffness ratios ($T_0=T_L=0.1$), respectively. As well, for the moderate stiffness ratios ($T_0=T_L=10$) in case 3, increasing α_0 from 0.0 to 1.0, causes reduce in the values of Ω_i ($i=1,2,3,4$) of the NAFG beam from 2.0948, 3.2328, 5.5103 and 8.8167, and approach 1.6202, 2.8681, 4.6347 and 7.9149, respectively. Moreover, when the end mass ratio α_0 in this case changes, the first four dimensionless natural frequency coefficients of the NAFG beam remain almost constant for the high stiffness ratios ($T_0=T_L=10^5$). In other words, this latter state corresponds to a pinned–pinned beam, and obviously, the effect of α_0 on the natural frequencies of the beam is very negligible.

From Fig. 8 and Table 8, it is concluded that increasing the end mass ratio α_0 always causes decrease in the values of Ω_i ($i=1,2,3,4$) for the beam, regardless of the amounts of the stiffness ratios. On the average and based on the amounts of Ω_i ($i=1,2,3,4$), Ω_4 and Ω_3 of this case have the lowest and highest sensitivity with respect to the variation of the end mass ratio, respectively. However, the second dimensionless natural frequency coefficient in the case 3 can reduce by nearly 28% whenever the end mass ratio α_0 increases from 0.0 to 1.0 for $T_0=T_L=100$. On the other hand, by increasing in the stiffness ratios, Ω_i ($i=1,2,3,4$) of the beam always increase, irrespective of the value of the end mass ratio. At the most sensitive state, increasing T_0 and T_L from the low stiffness ratios ($T_0=T_L=0.1$) to the high stiffness ratios ($T_0=T_L=10^5$) for $\alpha_0=1.0$, can raise the quantity of Ω_2 for the NAFG beam in case 3 by about 7.2 times.

Case 4

Based on data shown in Table 9, it is founded the free-guided supported NAFG beam with two translational springs at $x=0$ and $x=L$, and attached point mass at $x=0$ (Fig. 5d), when the end mass ratio α_0 increases from 0.0 up to 1.0, the first four dimensionless natural frequency coefficients of the NAFG beam decrease from 0.7864, 2.9795, 6.2937 and 9.7279, and tend to 0.6944, 2.1862, 5.4114 and 8.8400 for the low stiffness ratios ($T_0=T_L=0.1$), respectively. Also, for the moderate stiffness ratios ($T_0=T_L=10$) in case 4, increasing α_0 from 0.0 to 1.0, causes reduce in the values of Ω_i ($i=1,2,3,4$) of the NAFG beam from 2.4178, 3.4960, 6.3757 and 9.7506, and approach 1.9114, 2.8715, 5.4761 and 8.8547, respectively. Furthermore, as the end mass ratio α_0 in this case varies, the first four dimensionless natural frequency coefficients of the NAFG beam stay almost constant for the high stiffness ratios ($T_0=T_L=10^5$). In other words, this latter state corresponds to a pinned-fixed beam, and evidently, the effect of α_0 on the natural frequencies of the beam is very insignificant.

According to Fig. 9 and Table 9, it is observed that increasing the end mass ratio α_0 always causes a reduction in the values of Ω_i ($i=1,2,3,4$) for the beam, regardless of the quantities of the stiffness ratios. On the average and concerning the quantities of Ω_i ($i=1,2,3,4$), changing of the end mass ratio α_0 has the minimum and maximum effects on the values of Ω_4 and Ω_2 for this case, respectively. Accordingly, the second dimensionless natural frequency coefficient in case 4 can reduce by about 28% whenever the end mass ratio α_0 increases from 0.0 to 1.0 for $T_0=T_L=500$. On the other hand, by increasing the stiffness ratios, Ω_i ($i=1,2,3,4$) of the beam always increases, irrespective of the amount of the end mass ratio. At the most sensitive state, increasing T_0 and T_L from the low stiffness ratios ($T_0=T_L=0.1$) to the high stiffness ratios ($T_0=T_L=10^5$) for $\alpha_0=1.0$, can raise the quantity of Ω_1 for the NAFG beam in case 4 by nearly 6.5 times.

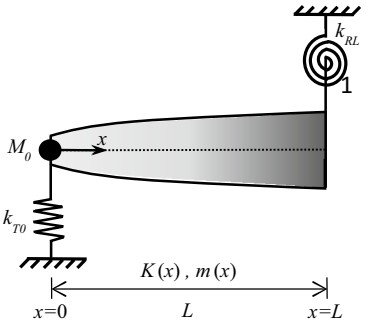

(a) Case 1 (α_0 = var., $T_0 = R_L$ = var., $\alpha_L = 0$, $R_0 = T_L = 0$, $p = 2$ and $c = 0.5$)

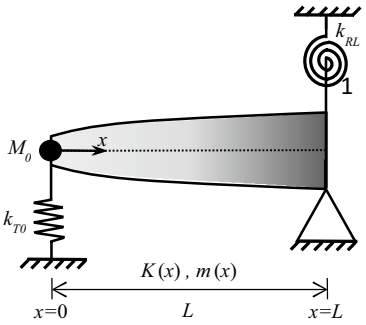

(b) Case 2 (α_0 = var., $T_0 = R_L$ = var., $\alpha_L = 0$, $R_0 = 0$, $T_L = \infty$, $p = 2$ and $c = 0.5$)

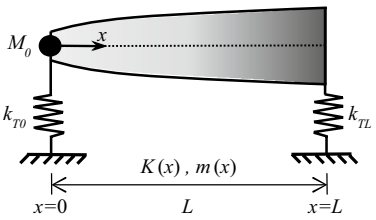

(c) Case 3 (α_0 = var., $T_0 = T_L$ = var., $\alpha_L = 0$, $R_0 = R_L = 0$, $p = 2$ and $c = 0.5$)

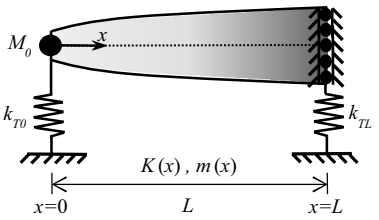

(d) Case 4 (α_0 = var., $T_0 = T_L$ = var., $\alpha_L = 0$, $R_0 = 0$, $R_L = \infty$, $p = 2$ and $c = 0.5$)

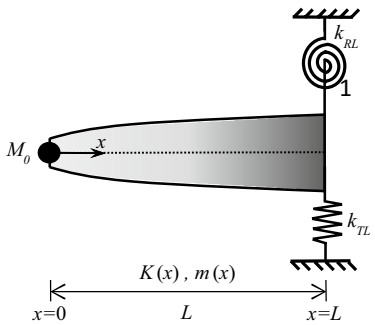

(e) Case 5 (α_0 = var., $R_L = T_L$ = var., $\alpha_L = 0$, $R_0 = T_0 = 0$, $p = 2$ and $c = 0.5$)

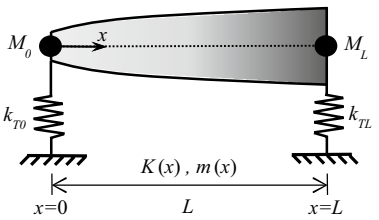

(f) Case 6 ($\alpha_0 = \alpha_L$ = var., $T_0 = T_L$ = var., $R_0 = R_L = 0$, $p = 2$ and $c = 0.5$)

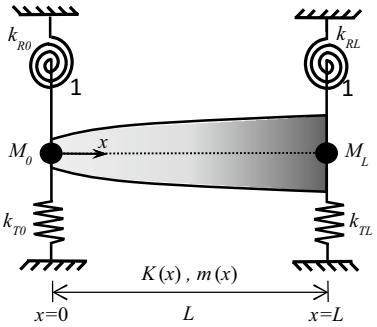

(g) Case 7 ($\alpha_0 = \alpha_L$ = var., $R_0 = T_0 = R_L = T_L$ = var., $p = 2$ and $c = 0.5$)

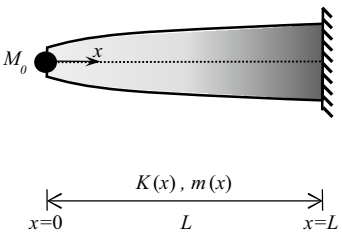

(h) Case 8 (p = var., c = var., α_0 = var., $\alpha_L = 0$, $R_0 = T_0 = 0$ and $R_L = T_L = \infty$)

Fig. 5 Schematic of the NAFG beams with end point masses and different boundary conditions in parametric studies

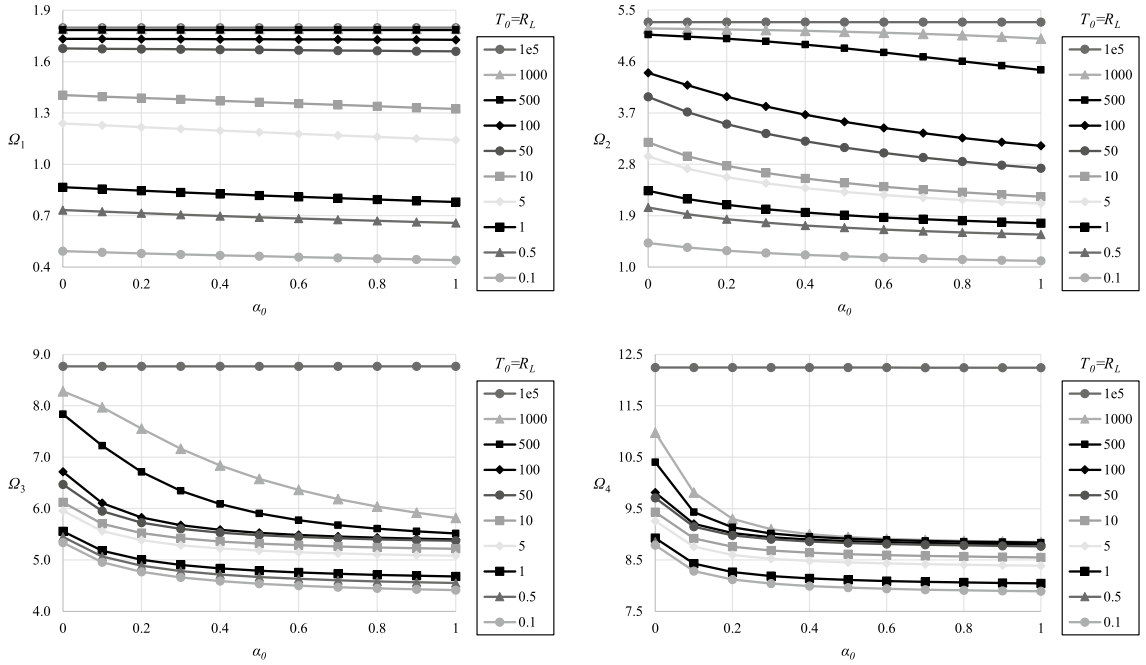

Fig. 6 Plot first four dimensionless natural frequency coefficients Ω_i, $i=1,2,3,4$ for Case 1

By comparing the results of Tables 6, 7, 8 and 9 (i.e., cases 1 to 4), it is concluded that the effect of the translational springs on the natural frequencies of the NAFG is more significant than the rotational springs, regardless of the attached tip mass. In other words, the sensitivity of the natural frequencies to the variation of the translational stiffness ratios is greater than the rotational stiffness ratios.

Case 5

By observing data in Table 10, it is founded that for the free supported NAFG beam with the translational and rotational springs at $x=L$, and attached point mass at $x=0$ (Fig. 5e), as the end mass ratio α_0 increases from 0.0 up to 1.0, the first four dimensionless natural frequency coefficients of

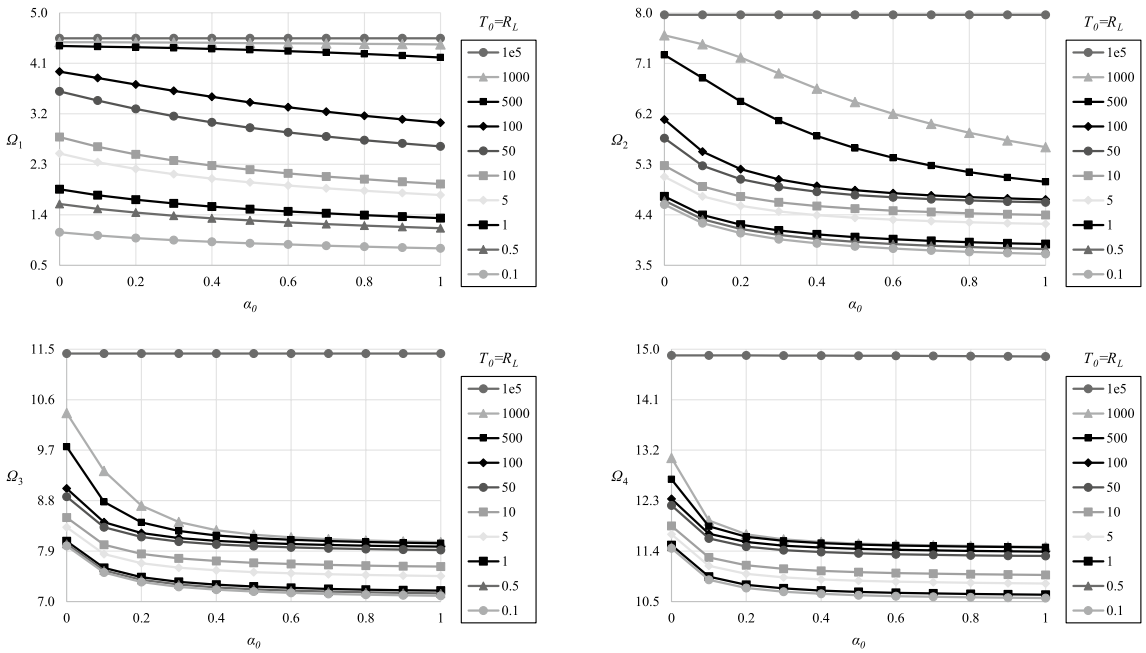

Fig. 7 Plot first four dimensionless natural frequency coefficients Ω_i, $i=1,2,3,4$ for Case 2

Table 6 First four dimensionless natural frequency coefficients Ω_i, $i=1,2,3,4$ for Case 1

α_0	Ω_i	$T_0=R_L$					
		0.1	1	10	100	1000	10^5
0.0	$i=1$	0.492952	0.866886	1.404016	1.732942	1.791404	1.798351
	$i=2$	1.421247	2.336679	3.185312	4.403371	5.179166	5.288310
	$i=3$	5.335832	5.557965	6.120736	6.715555	8.279303	8.765565
	$i=4$	8.787956	8.927485	9.430971	9.811960	10.979512	12.245030
0.1	$i=1$	0.486356	0.856236	1.395802	1.732434	1.791397	1.798351
	$i=2$	1.343338	2.190989	2.943223	4.185226	5.170829	5.288309
	$i=3$	4.953359	5.179385	5.704170	6.105940	7.969153	8.765539
	$i=4$	8.285159	8.428002	8.917889	9.202804	9.813164	12.244762
0.2	$i=1$	0.480138	0.846105	1.387580	1.731919	1.791391	1.798351
	$i=2$	1.288386	2.089626	2.774272	3.985315	5.161263	5.288308
	$i=3$	4.768110	5.002410	5.522263	5.825075	7.555406	8.765512
	$i=4$	8.119675	8.266029	8.759370	9.024212	9.301706	12.244481
0.3	$i=1$	0.474266	0.836460	1.379368	1.731397	1.791384	1.798351
	$i=2$	1.247130	2.014404	2.648908	3.813462	5.150219	5.288307
	$i=3$	4.659421	4.901050	5.422567	5.676221	7.164308	8.765485
	$i=4$	8.039379	8.187940	8.684473	8.942778	9.098284	12.244187
0.4	$i=1$	0.468710	0.827267	1.371180	1.730867	1.791377	1.798351
	$i=2$	1.214818	1.956027	2.551513	3.667859	5.137401	5.288306
	$i=3$	4.587982	4.835557	5.360023	5.587057	6.840265	8.765458
	$i=4$	7.992194	8.142212	8.641077	8.896579	9.001369	12.243877
0.5	$i=1$	0.463442	0.818499	1.363030	1.730329	1.791371	1.798351
	$i=2$	1.188723	1.909221	2.473254	3.543875	5.122454	5.288305
	$i=3$	4.537438	4.789802	5.317238	5.528608	6.577361	8.765430
	$i=4$	7.961193	8.112233	8.612813	8.866899	8.946844	12.243553
0.6	$i=1$	0.458439	0.810125	1.354932	1.729783	1.791364	1.798351
	$i=2$	1.167150	1.870755	2.408756	3.437134	5.104972	5.288304
	$i=3$	4.499786	4.756048	5.286166	5.487670	6.362736	8.765403
	$i=4$	7.939285	8.091078	8.592956	8.846247	8.912386	12.243211
0.7	$i=1$	0.453680	0.802120	1.346897	1.729229	1.791357	1.798351
	$i=2$	1.148985	1.838522	2.354548	3.344135	5.084510	5.288304
	$i=3$	4.470647	4.730129	5.262594	5.457534	6.185948	8.765374
	$i=4$	7.922987	8.075357	8.578247	8.831055	8.888787	12.242851
0.8	$i=1$	0.449145	0.794458	1.338935	1.728667	1.791351	1.798351
	$i=2$	1.133458	1.811085	2.308274	3.262195	5.060628	5.288303
	$i=3$	4.447426	4.709603	5.244106	5.434486	6.039484	8.765346
	$i=4$	7.910391	8.063217	8.566916	8.819416	8.871664	12.242471
0.9	$i=1$	0.444817	0.787119	1.331057	1.728096	1.791344	1.798351
	$i=2$	1.120021	1.787425	2.268269	3.189274	5.032954	5.288302
	$i=3$	4.428484	4.692947	5.229221	5.416317	5.917978	8.765317
	$i=4$	7.900366	8.053561	8.55792	8.810214	8.858695	12.24207
1.0	$i=1$	0.440681	0.780079	1.323269	1.727517	1.791337	1.798351
	$i=2$	1.108270	1.766798	2.233320	3.123802	5.001279	5.288301
	$i=3$	4.412739	4.679163	5.216983	5.401643	5.817447	8.765287
	$i=4$	7.892198	8.045698	8.550605	8.802759	8.848542	12.241646

the NAFG beam decrease from 0.7174, 1.4647, 5.3364 and 8.7881, and tend to 0.6026, 1.2149, 4.4150 and 7.8926 for the low stiffness ratios ($R_L=T_L=0.1$), respectively. In addition, for the moderate stiffness ratios ($R_L=T_L=10$) in case 5, increasing α_0 from 0.0 to 1.0, causes reduce in the values of Ω_i ($i=1,2,3,4$) of the NAFG beam from 2.0450, 3.2691, 6.1357 and 9.4364, and approach 1.5175, 2.8583, 5.3094 and 8.5744, respectively. Besides, when the end mass ratio

Table 7 First four dimensionless natural frequency coefficients Ω_i, $i=1,2,3,4$ for Case 2

α_0	Ω_i	$T_0=R_L$					
		0.1	1	10	100	1000	10^5
0.0	$i=1$	1.086947	1.853565	2.786607	3.950757	4.477375	4.546696
	$i=2$	4.584865	4.729431	5.276481	6.099570	7.601809	7.965140
	$i=3$	7.993467	8.075544	8.498378	9.017535	10.362548	11.424005
	$i=4$	11.451488	11.507588	11.850990	12.329871	13.062259	14.890699
0.1	$i=1$	1.030341	1.749222	2.611414	3.839483	4.474622	4.546696
	$i=2$	4.250563	4.396180	4.904843	5.526696	7.442037	7.965127
	$i=3$	7.517835	7.601384	8.013731	8.414859	9.330434	11.423841
	$i=4$	10.889682	10.947114	11.289602	11.711207	11.945292	14.889624
0.2	$i=1$	0.985890	1.668037	2.475605	3.722711	4.471647	4.546696
	$i=2$	4.074429	4.224818	4.725622	5.213575	7.203436	7.965113
	$i=3$	7.348840	7.434500	7.850616	8.223928	8.712604	11.423671
	$i=4$	10.742221	10.800748	11.147281	11.562834	11.700075	14.888431
0.3	$i=1$	0.949595	1.602372	2.367138	3.608526	4.468424	4.546696
	$i=2$	3.965884	4.121183	4.622427	5.031070	6.922284	7.965099
	$i=3$	7.264238	7.351341	7.771049	8.135053	8.418793	11.423494
	$i=4$	10.676131	10.735264	11.084244	11.498611	11.608987	14.887100
0.4	$i=1$	0.919111	1.547684	2.278006	3.501813	4.464924	4.546695
	$i=2$	3.892209	4.051857	4.555861	4.916588	6.650440	7.965085
	$i=3$	7.213699	7.301794	7.724204	8.084235	8.273991	11.423312
	$i=4$	10.638791	10.698299	11.048835	11.462956	11.562563	14.885605
0.5	$i=1$	0.892957	1.501101	2.202999	3.404390	4.461114	4.546695
	$i=2$	3.838881	4.002251	4.509528	4.840122	6.409567	7.965071
	$i=3$	7.180157	7.268965	7.693400	8.051463	8.194370	11.423122
	$i=4$	10.614825	10.674586	11.026186	11.440311	11.534590	14.883915
0.6	$i=1$	0.870140	1.460712	2.138645	3.316285	4.456955	4.546695
	$i=2$	3.798471	3.965009	4.475486	4.786310	6.201187	7.965057
	$i=3$	7.156291	7.245634	7.671622	8.028612	8.145660	11.422926
	$i=4$	10.598148	10.658091	11.010461	11.424664	11.515933	14.881989
0.7	$i=1$	0.849965	1.425188	2.082551	3.236750	4.452405	4.546694
	$i=2$	3.766781	3.936026	4.449445	4.746778	6.021036	7.965043
	$i=3$	7.138449	7.228207	7.655417	8.011782	8.113267	11.422722
	$i=4$	10.585878	10.645958	10.998909	11.413209	11.502616	14.879774
0.8	$i=1$	0.831929	1.393574	2.033016	3.164804	4.447413	4.546694
	$i=2$	3.741256	3.912831	4.428896	4.716698	5.864281	7.965029
	$i=3$	7.124608	7.214698	7.642892	7.998876	8.090334	11.422509
	$i=4$	10.576473	10.636659	10.990066	11.404462	11.492639	14.877202
0.9	$i=1$	0.815655	1.365163	1.988795	3.099473	4.441923	4.546694
	$i=2$	3.720254	3.893850	4.412275	4.693138	5.726798	7.965014
	$i=3$	7.113561	7.203921	7.632922	7.988668	8.073310	11.422288
	$i=4$	10.569035	10.629306	10.983078	11.397564	11.484887	14.874180
1.0	$i=1$	0.800857	1.339417	1.948954	3.039880	4.435872	4.546694
	$i=2$	3.702667	3.878029	4.398559	4.674236	5.605309	7.965000
	$i=3$	7.104539	7.195123	7.624798	7.980393	8.060202	11.422059
	$i=4$	10.563005	10.623346	10.977419	11.391986	11.478692	14.870582

α_0, in this case, increases from 0.0 up to 1.0, the first four dimensionless natural frequency coefficients of the NAFG beam decrease from 2.4937, 5.5291, 8.9233 and 12.3591, and tend to 1.6868, 4.6819, 8.0428 and 11.4774 for the high stiffness ratios ($R_L=T_L=10^5$), respectively. This latter state corresponds to a free-clamped beam, and clearly, the effect of α_0 on the natural frequencies of the beam is significant for this case.

Table 8 First four dimensionless natural frequency coefficients Ω_i, $i=1,2,3,4$ for Case 3

α_0	Ω_i	$T_0=T_L$					
		0.1	1	10	100	1000	10^5
0.0	$i=1$	0.680777	1.207542	2.094774	3.099660	3.430093	3.474321
	$i=2$	1.041079	1.848213	3.232774	5.154749	6.684785	7.000638
	$i=3$	5.305762	5.324498	5.510301	6.873084	9.438575	10.487663
	$i=4$	8.770339	8.774522	8.816701	9.260531	11.775333	13.966329
0.1	$i=1$	0.650939	1.155535	2.019141	3.074849	3.429591	3.474321
	$i=2$	1.016500	1.802904	3.123483	4.794855	6.628881	7.000632
	$i=3$	4.921946	4.940368	5.128358	6.478026	8.757783	10.487572
	$i=4$	8.266864	8.270501	8.307540	8.727401	10.741093	13.965648
0.2	$i=1$	0.625984	1.111780	1.951892	3.047748	3.429075	3.474321
	$i=2$	1.001600	1.775174	3.051364	4.512309	6.549470	7.000627
	$i=3$	4.735044	4.753902	4.950000	6.317574	8.131351	10.487479
	$i=4$	8.100841	8.104440	8.141232	8.569501	10.439332	13.964912
0.3	$i=1$	0.604840	1.074567	1.892510	3.018510	3.428546	3.474321
	$i=2$	0.991699	1.756663	3.001630	4.303171	6.440468	7.000621
	$i=3$	4.624974	4.644434	4.849092	6.238946	7.716564	10.487383
	$i=4$	8.020217	8.023844	8.060988	8.497953	10.329986	13.964112
0.4	$i=1$	0.586662	1.042493	1.839996	2.987408	3.428001	3.474321
	$i=2$	0.984680	1.743506	2.965787	4.146508	6.303621	7.000615
	$i=3$	4.552431	4.572474	4.784704	6.193565	7.459409	10.487285
	$i=4$	7.972819	7.976479	8.013999	8.457584	10.276238	13.963240
0.5	$i=1$	0.570818	1.014490	1.793317	2.954822	3.427442	3.474321
	$i=2$	0.979459	1.733707	2.938950	4.026684	6.150782	7.000609
	$i=3$	4.501000	4.521563	4.740211	6.164324	7.303173	10.487185
	$i=4$	7.941670	7.945359	7.983201	8.431753	10.244679	13.962286
0.6	$i=1$	0.556842	0.989757	1.751555	2.921198	3.426867	3.474321
	$i=2$	0.975432	1.726141	2.918209	3.933316	5.995942	7.000604
	$i=3$	4.462625	4.483642	4.707689	6.144004	7.206780	10.487082
	$i=4$	7.919652	7.923366	7.961473	8.413832	10.224012	13.961238
0.7	$i=1$	0.544383	0.967691	1.713938	2.887000	3.426275	3.474321
	$i=2$	0.972235	1.720131	2.901750	3.859423	5.848057	7.000598
	$i=3$	4.432888	4.454299	4.682909	6.129096	7.144727	10.486976
	$i=4$	7.903271	7.907004	7.945330	8.400680	10.209458	13.960081
0.8	$i=1$	0.533177	0.947828	1.679836	2.852664	3.425667	3.474321
	$i=2$	0.969637	1.715246	2.888401	3.800151	5.710842	7.000592
	$i=3$	4.409165	4.430918	4.663413	6.117707	7.102692	10.486867
	$i=4$	7.890609	7.894360	7.932866	8.390622	10.198664	13.958797
0.9	$i=1$	0.523017	0.929812	1.648732	2.818567	3.425040	3.474321
	$i=2$	0.967485	1.711200	2.877372	3.752027	5.585030	7.000586
	$i=3$	4.389797	4.411849	4.647682	6.108728	7.072824	10.486755
	$i=4$	7.880531	7.884296	7.922954	8.382682	10.190345	13.957366
1.0	$i=1$	0.513743	0.913361	1.620206	2.785012	3.424395	3.474321
	$i=2$	0.965675	1.707795	2.868117	3.712512	5.470049	7.000580
	$i=3$	4.373685	4.395999	4.634725	6.101472	7.050713	10.486641
	$i=4$	7.872319	7.876096	7.914883	8.376255	10.183739	13.955759

As seen in Fig. 10 and Table 10, it is observed that increasing the end mass ratio α_0 always causes a decrease in the values of Ω_i ($i=1,2,3,4$) for the beam, regardless of the quantities of the stiffness ratios. On average and based on the amounts of Ω_i ($i=1,2,3,4$), Ω_4 and Ω_1, in this case, have the lowest and highest sensitivity to the variation of the end mass ratio, respectively. Accordingly, the first dimensionless natural frequency coefficient in case 5 can reduce by

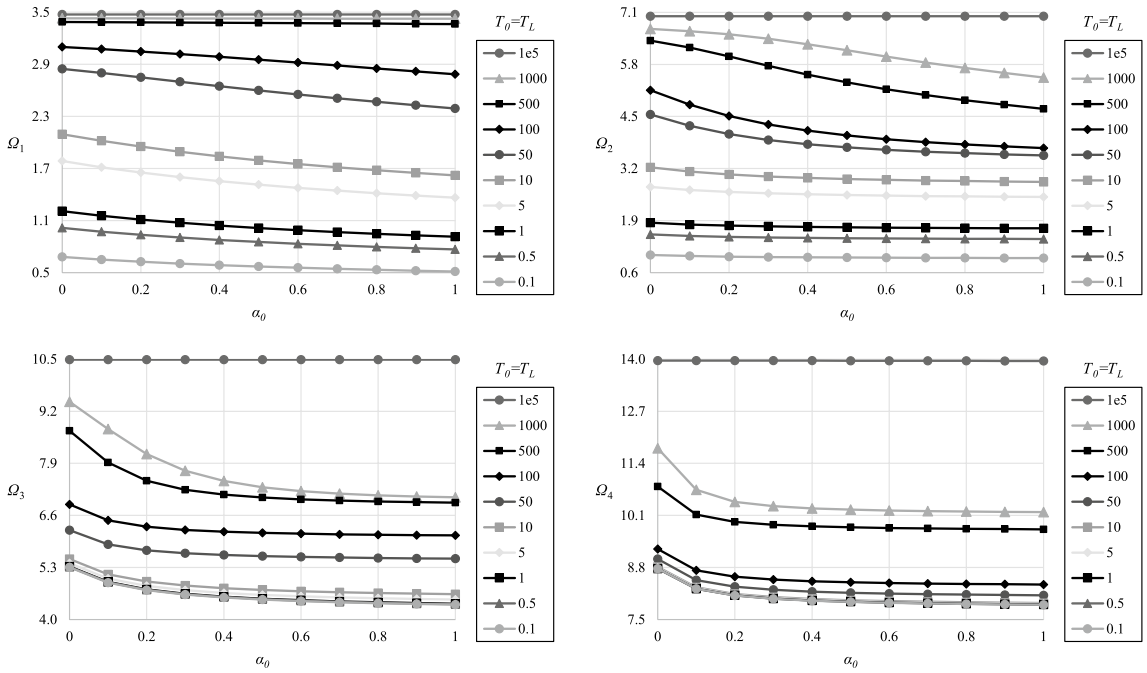

Fig. 8 Plot first four dimensionless natural frequency coefficients Ω_i, $i=1,2,3,4$ for Case 3

nearly 32% whenever the end mass ratio α_0 increases from 0.0 to 1.0 for $R_L=T_L=10^5$. On the other hand, by increasing the stiffness ratios, Ω_i ($i=1,2,3,4$) of the beam always increases, irrespective of the value of the end mass ratio. At the most sensitive state, increasing R_L and T_L from the low stiffness ratios ($R_L=T_L=0.1$) to the high stiffness ratios ($R_L=T_L=10^5$) for $\alpha_0=1.0$, can raise the quantity of Ω_2 for the NAFG beam in case 5 by about 3.9 times.

Case 6

From data reported in Table 11, it is concluded that for the free supported NAFG beam with two translational springs and two attached point masses at $x=0$ and $x=L$ (Fig. 5f), as the end mass ratios $\alpha_0=\alpha_L$ increase from 0.0 up to 1.0, the first four dimensionless natural frequency coefficients of the NAFG beam decrease from 0.6808, 1.0411, 5.3058 and 8.7703, and tend to 0.5136, 0.7533, 3.8761 and 7.2400 for the low stiffness ratios ($T_0=T_L=0.1$), respectively. As well, for the moderate stiffness ratios ($T_0=T_L=10$) in case 6, increasing $\alpha_0=\alpha_L$ from 0.0 to 1.0, cause reduce in the values of Ω_i ($i=1,2,3,4$) of the NAFG beam from 2.0948, 3.2328, 5.5103 and 8.8167, and approach 1.6197, 2.3621, 3.9183 and 7.2425, respectively. Moreover, when the end mass ratios $\alpha_0=\alpha_L$ in this case change, the first four dimensionless natural frequency coefficients of the NAFG beam remain almost constant for the high stiffness ratios ($T_0=T_L=10^5$). In other words, this latter state corresponds to a pinned–pinned beam, and obviously, the effect of α_0 and α_L on the natural frequencies of the beam are very negligible.

From Fig. 11 and Table 11, it is observed that increasing the end mass ratios $\alpha_0=\alpha_L$ always causes a reduction in the values of Ω_i ($i=1,2,3,4$) for the beam, regardless of the quantities of the stiffness ratios. On average and about the quantities of Ω_i ($i=1,2,3,4$), changing of the end mass ratios $\alpha_0=\alpha_L$ have the lowest and highest effect on the values of Ω_1 and Ω_3 in this case, respectively. Accordingly, the third dimensionless natural frequency coefficient in case 6 can reduce by nearly 33% whenever the end mass ratios $\alpha_0=\alpha_L$ increase from 0.0 to 1.0 for $T_0=T_L=50$. On the other hand, by increasing the stiffness ratios, Ω_i ($i=1,2,3,4$) of the beam always increases, irrespective of the values of the end mass ratios. At the most sensitive state, increasing T_0 and T_L from the low stiffness ratios ($T_0=T_L=0.1$) to the high stiffness ratios ($T_0=T_L=10^5$) for $\alpha_0=\alpha_L=1.0$, can raise the quantity of Ω_2 for the NAFG beam in case 6 by about 9.3 times.

Effects of the Symmetric Elastic Boundary Conditions with End Masses (Case 7)

The effects of the non-classical symmetric rotational and translational stiffness ratios (i.e., R_0, T_0, R_L, and T_L) with end mass ratios (i.e., α_0 and α_L), on the first four dimensionless natural frequency coefficients Ω_i ($i=1,2,3,4$) for the NAFG beam ($p=2$, $c=0.5$) introduced as case 7 are depicted in Fig. 12. Moreover, the corresponding numerical values of Ω_i ($i=1,2,3,4$) for this case are arranged in Tables 12.

Table 9 First four dimensionless natural frequency coefficients Ω_i, $i=1,2,3,4$ for Case 4

α_0	Ω_i	$T_0=T_L$					
		0.1	1	10	100	1000	10^5
0.0	$i=1$	0.786362	1.394196	2.417790	3.768180	4.441236	4.546306
	$i=2$	2.979499	3.037363	3.495958	5.227826	7.380717	7.962557
	$i=3$	6.293701	6.301177	6.375697	7.060569	9.751203	11.415886
	$i=4$	9.727917	9.729973	9.750594	9.961668	11.795283	14.872063
0.1	$i=1$	0.774296	1.370968	2.356023	3.700761	4.438720	4.546306
	$i=2$	2.755013	2.812969	3.274784	4.924532	7.265749	7.962543
	$i=3$	5.880682	5.886787	5.948369	6.559193	9.030947	11.415723
	$i=4$	9.204771	9.206215	9.220740	9.374329	10.870579	14.871002
0.2	$i=1$	0.763065	1.348904	2.292578	3.622372	4.436006	4.546305
	$i=2$	2.608931	2.668255	3.142262	4.698135	7.085937	7.962530
	$i=3$	5.704838	5.710538	5.768453	6.366119	8.450009	11.415554
	$i=4$	9.046640	9.047979	9.061479	9.206279	10.627713	14.869825
0.3	$i=1$	0.752577	1.327998	2.230791	3.537439	4.433074	4.546305
	$i=2$	2.505181	2.566718	3.058265	4.545896	6.852090	7.962516
	$i=3$	5.609025	5.614612	5.671654	6.273801	8.139344	11.415379
	$i=4$	8.972344	8.973660	8.986933	9.130310	10.542003	14.868513
0.4	$i=1$	0.742749	1.308218	2.172648	3.451147	4.429896	4.546305
	$i=2$	2.427091	2.491325	3.002146	4.444451	6.606597	7.962502
	$i=3$	5.548978	5.554547	5.611582	6.221320	7.981949	11.415198
	$i=4$	8.929396	8.930708	8.943936	9.087389	10.499982	14.867040
0.5	$i=1$	0.733512	1.289512	2.118948	3.367472	4.426446	4.546304
	$i=2$	2.365872	2.433051	2.962853	4.375355	6.379077	7.962488
	$i=3$	5.507885	5.513469	5.570777	6.187850	7.896533	11.415010
	$i=4$	8.901457	8.902769	8.916006	9.059880	10.475279	14.865376
0.6	$i=1$	0.724809	1.271821	2.069766	3.288611	4.422689	4.546304
	$i=2$	2.316414	2.386638	2.934201	4.326740	6.177752	7.962474
	$i=3$	5.478017	5.483627	5.541289	6.164762	7.845401	11.414814
	$i=4$	8.881843	8.883157	8.896419	9.040768	10.459076	14.863481
0.7	$i=1$	0.716586	1.255081	2.024834	3.215403	4.418588	4.546304
	$i=2$	2.275523	2.348802	2.912575	4.291344	6.001564	7.962460
	$i=3$	5.455336	5.460975	5.518999	6.147916	7.812068	11.414612
	$i=4$	8.867320	8.868636	8.881927	9.026725	10.447646	14.861304
0.8	$i=1$	0.708799	1.239227	1.983748	3.147896	4.414101	4.546304
	$i=2$	2.241088	2.317372	2.895771	4.264736	5.847124	7.962446
	$i=3$	5.437530	5.443199	5.501566	6.135101	7.788851	11.414401
	$i=4$	8.856135	8.857455	8.870773	9.015973	10.439157	14.858779
0.9	$i=1$	0.701410	1.224197	1.946085	3.085765	4.409179	4.546303
	$i=2$	2.211652	2.290860	2.882389	4.244161	5.710991	7.962431
	$i=3$	5.423184	5.428879	5.487562	6.125034	7.771841	11.414182
	$i=4$	8.847258	8.848580	8.861924	9.007479	10.432608	14.855816
1.0	$i=1$	0.694383	1.209931	1.911445	3.028539	4.403767	4.546303
	$i=2$	2.186176	2.268203	2.871510	4.227857	5.590234	7.962417
	$i=3$	5.411378	5.417099	5.476067	6.116919	7.758880	11.413954
	$i=4$	8.840042	8.841366	8.854733	9.000600	10.427402	14.852294

Based on data shown in Table 12, it is concluded for the symmetric elastic-supported NAFG beam with two translational and rotational springs at $x=0$ and at $x=L$, and attached point masses at $x=0$ and at $x=L$ (Fig. 5g), when the all stiffness ratios $R_0=T_0=R_L=T_L$ increase from 0.1 (corresponding to low stiffness) up to 10^5 (corresponding to high stiffness), the first four dimensionless natural frequency coefficients of the NAFG beam without end masses

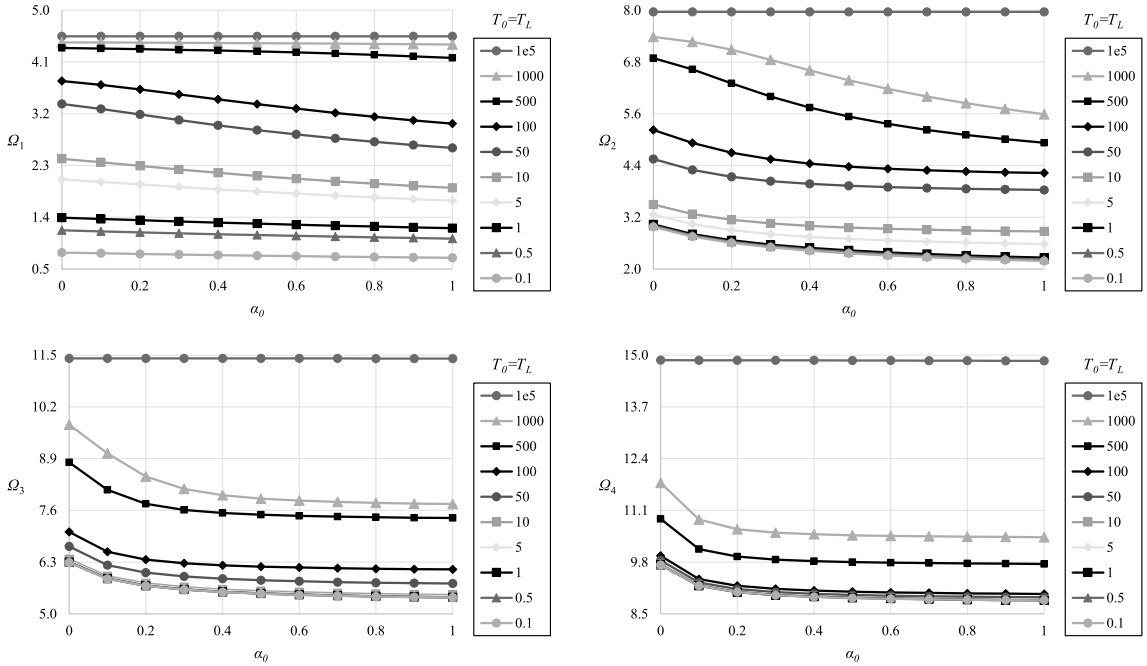

Fig. 9 Plot first four dimensionless natural frequency coefficients Ω_i, $i=1,2,3,4$ for Case 4

(i.e., $\alpha_0=\alpha_L=0$) increase considerably from 0.7735, 1.5413, 5.3511 and 8.7984, and tend to 5.2687, 8.7315, 12.2044 and 15.6604, respectively. Also, for the end mass ratios $\alpha_0=\alpha_L=1.0$ in case 7, increasing $R_0=T_0=R_L=T_L$ from 0.1 to 10^5, cause raise in the values of Ω_i ($i=1,2,3,4$) of the NAFG beam from 0.6266, 1.0391, 3.9183 and 7.2606, and approach 5.2687, 8.7309, 12.1974 and 15.5840, respectively. Note that, in Table 12, the results from [1] are given in square brackets.

According to Fig. 12 and Table 12, it is observed that increasing all stiffness ratios always causes an increase in the values of Ω_i ($i=1,2,3,4$) for the beam, regardless of the quantities of the end mass ratios. Based on the slope of the Ω_i–stiffness ratios curves, in this case, Ω_4 and Ω_1 have the lowest and highest sensitivity versus the simultaneous change of the stiffness ratios, respectively. Accordingly, increasing $R_0=T_0=R_L=T_L$ from the low stiffness ratios (i.e., 0.1) to the high stiffness ratios (i.e., 10^5) for $\alpha_0=1.0$, can raise the quantity of Ω_1 for the NAFG beam in case 7 by about 8.4 times. On the other hand, by increasing the end mass ratios, Ω_i ($i=1,2,3,4$) of the beam always decreases, irrespective of the amount of the stiffness ratios. On average, the first and second dimensionless natural frequency coefficients in case 7 have the lowest and highest variation versus the changing of the end mass ratios, respectively. At the most sensitive state, the quantity of Ω_2 for the NAFG beam in the case 7 can reduce by nearly 33% whenever the end mass ratios $\alpha_0=\alpha_L$ increase from 0.0 to 1.0 for $R_0=T_0=R_L=T_L=0.1$.

Effects of the NAFG Parameters with End Mass (Case 8)

In Figs. 13 and 14, changing of the first four dimensionless natural frequency coefficients Ω_i ($i=1,2,3,4$) for the NAFG beam introduced as case 8 to the variation of the NAFG parameters, namely, the gradient index p and gradient coefficient c are investigated, respectively. Moreover, in Tables 13 and 14, the corresponding numerical values of Ω_i ($i=1,2,3,4$) for this case are presented, respectively.

By observing data in Table 13, it is founded that for the free-fixed supported NAFG beam with the translational and rotational springs at $x=0$, and attached point mass at $x=0$ (Fig. 5h), whereas the gradient index p increases from -1 up to 3, the first four dimensionless natural frequency coefficients of the NAFG beam without end masses (i.e., $\alpha_0=\alpha_L=0$) increase from 2.0836, 5.2238, 8.7390 and 12.2324, and tend to 2.6398, 5.6361, 8.9967 and 12.4216, respectively. In addition, for the end mass ratio $\alpha_0=1.0$ in case 8, increasing p from -1 to 3, causes an increase in the values of Ω_i ($i=1,2,3,4$) of the NAFG beam from 1.3563, 4.4770, 7.9310 and 11.4057, and approach 1.8079, 4.7539, 8.0905 and 11.5185, respectively. Note that, in Table 13, the results from [1] are given in square brackets.

As seen in Fig. 13 and Table 13, it is observed that increasing the gradient index p always causes an increase linearly in the values of Ω_i ($i=1,2,3,4$) for the beam, regardless of the quantity of the end mass ratio. This effect is more pronounced for the first natural frequency of the NAFG

Table 10 First four dimensionless natural frequency coefficients Ω_i, $i=1,2,3,4$ for Case 5

α_0	Ω_i	$R_L=T_L$					
		0.1	1	10	100	1000	10^5
0.0	$i=1$	0.717392	1.263346	2.045010	2.436468	2.487953	2.493687
	$i=2$	1.464700	2.402279	3.269137	4.671098	5.439950	5.529123
	$i=3$	5.336445	5.563254	6.135678	6.751019	8.472788	8.923314
	$i=4$	8.788093	8.928778	9.436368	9.813393	11.057142	12.359129
0.1	$i=1$	0.701276	1.231676	1.951258	2.263075	2.302045	2.306384
	$i=2$	1.397066	2.279157	3.122039	4.479812	5.091026	5.158844
	$i=3$	4.954523	5.189413	5.752133	6.424900	8.065602	8.425192
	$i=4$	8.285453	8.430766	8.934812	9.313832	10.658500	11.784370
0.2	$i=1$	0.686522	1.202713	1.871746	2.135359	2.167651	2.171251
	$i=2$	1.351095	2.198196	3.038250	4.377739	4.927572	4.988119
	$i=3$	4.769614	5.015173	5.586799	6.299489	7.925526	8.263346
	$i=4$	8.120021	8.269272	8.779618	9.165320	10.551590	11.643466
0.3	$i=1$	0.672988	1.176246	1.804231	2.036164	2.064348	2.067494
	$i=2$	1.317735	2.141112	2.985348	4.315814	4.834202	4.891218
	$i=3$	4.661149	4.915515	5.496363	6.235086	7.856714	8.185235
	$i=4$	8.039750	8.191402	8.706131	9.096065	10.503554	11.581599
0.4	$i=1$	0.660540	1.152029	1.746339	1.956006	1.981406	1.984244
	$i=2$	1.292409	2.098815	2.949313	4.274574	4.774055	4.829005
	$i=3$	4.589867	4.851169	5.439604	6.196193	7.816054	8.139463
	$i=4$	7.992578	8.145795	8.663491	9.056195	10.476401	11.546980
0.5	$i=1$	0.649051	1.129814	1.696103	1.889281	1.912662	1.915277
	$i=2$	1.272526	2.066289	2.923344	4.245238	4.732150	4.785748
	$i=3$	4.539439	4.806238	5.400737	6.170238	7.789258	8.109443
	$i=4$	7.961586	8.115893	8.635692	9.030324	10.458971	11.524884
0.6	$i=1$	0.638414	1.109370	1.652005	1.832461	1.854304	1.856749
	$i=2$	1.256507	2.040542	2.903807	4.223339	4.701306	4.753954
	$i=3$	4.501876	4.773102	5.372479	6.151711	7.770284	8.088253
	$i=4$	7.939684	8.094792	8.616147	9.012195	10.446844	11.509564
0.7	$i=1$	0.628533	1.090492	1.612884	1.783202	1.803829	1.806139
	$i=2$	1.243330	2.019683	2.888609	4.206384	4.677667	4.729609
	$i=3$	4.472808	4.747663	5.351020	6.137832	7.756150	8.072502
	$i=4$	7.923390	8.079109	8.601662	8.998788	10.437921	11.498321
0.8	$i=1$	0.619323	1.072999	1.577853	1.739879	1.759517	1.761718
	$i=2$	1.232305	2.002459	2.876467	4.192875	4.658978	4.710376
	$i=3$	4.449644	4.727521	5.334173	6.127052	7.745216	8.060337
	$i=4$	7.910798	8.066999	8.590498	8.988474	10.431082	11.489719
0.9	$i=1$	0.610714	1.056736	1.546226	1.701326	1.720139	1.722249
	$i=2$	1.222947	1.988008	2.866551	4.181863	4.643833	4.694800
	$i=3$	4.430750	4.711180	5.320600	6.118439	7.736507	8.050660
	$i=4$	7.900776	8.057366	8.581632	8.980294	10.425674	11.482927
1.0	$i=1$	0.602642	1.041565	1.517467	1.666678	1.684792	1.686824
	$i=2$	1.214907	1.975718	2.858307	4.172717	4.631314	4.681929
	$i=3$	4.415045	4.697657	5.309430	6.111401	7.729407	8.042778
	$i=4$	7.892610	8.049521	8.574421	8.973648	10.421290	11.477427

cantilever beam and negligible for the fourth natural frequency of one. In other words, based on the slope of the Ω_i–p curves, in this case, Ω_4 and Ω_1 have the lowest and highest sensitivity concerning the change of the gradient index, respectively. Accordingly, the first dimensionless natural frequency coefficient in case 8 with $c=0.5$, can increase by about 33% whenever the gradient index increases from -1 to 3 for $\alpha_0=1.0$. On the other hand, by increasing the

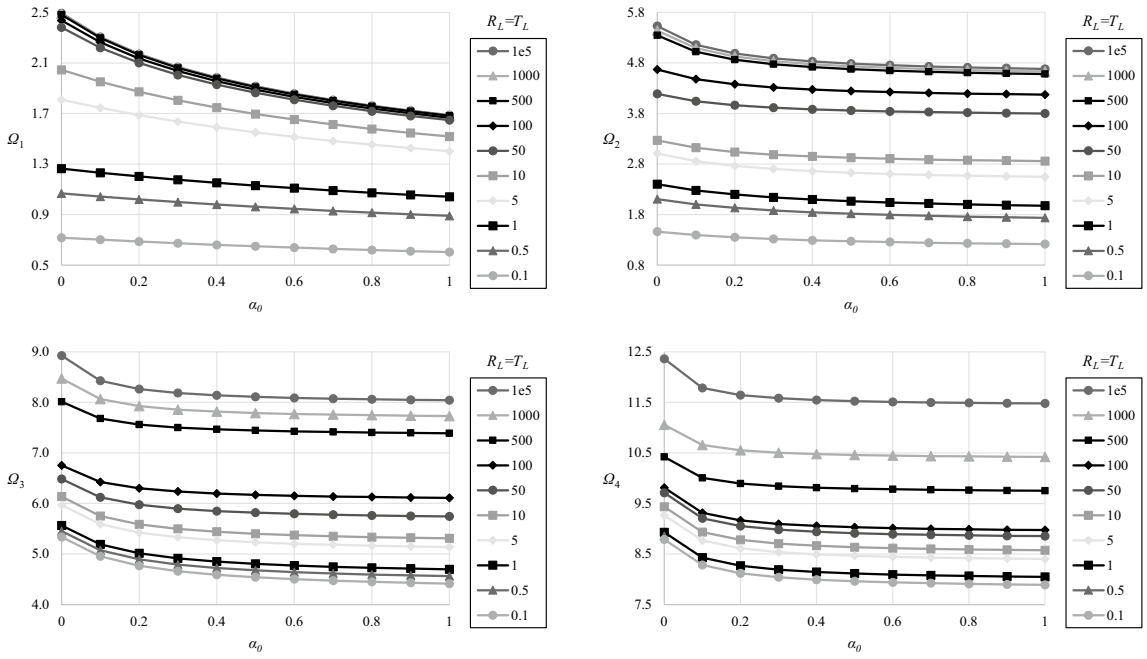

Fig. 10 Plot first four dimensionless natural frequency coefficients Ω_i, $i=1,2,3,4$ for Case 5

mass ratio α_0, Ω_i ($i=1,2,3,4$) of the beam always decreases, irrespective of the value of the gradient index. At the most sensitive state, increasing α_0 from 0.0 to 1.0 for $p=$-1 can reduce the quantity of Ω_1 for the NAFG beam in case 8 with $c=0.5$ by nearly 35%.

From data reported in Table 14, it is observed that for the free-fixed supported NAFG beam with the translational and rotational springs at $x=0$, and attached point mass at $x=0$ (Fig. 5h), whenever the gradient coefficient c increases from − 0.50 up to 0.50, the first four dimensionless natural frequency coefficients of the NAFG beam without end masses (i.e., $\alpha_0=\alpha_L=0$) increase from 1.1393, 3.6311, 6.5187 and 9.2575, and tend to 2.4937, 5.5300, 8.9272 and 12.3697, respectively. As well, for the end mass ratio $\alpha_0=1.0$ in case 8, increasing c from -0.50 to 0.50, causes an increase in the values of Ω_i ($i=1,2,3,4$) of the NAFG beam from 0.7445, 3.1768, 5.9856 and 8.6900, and approach 1.6868, 4.6824, 8.0456 and 11.4859, respectively. Note that, in Table 14, the results from [1] are given in square brackets.

From Fig. 14 and Table 14, it is concluded that increasing the gradient coefficient c always causes an increase almost linearly in the values of Ω_i ($i=1,2,3,4$) for the beam, regardless of the amount of the end mass ratio α_0. Based on the slope of the Ω_i–c curves, in this case, Ω_1 and Ω_4 have the lowest and highest sensitivity versus the change of the gradient coefficient, respectively. Accordingly, the four dimensionless natural frequency coefficient in case 8 with $p=2$ can increase by about 32% whenever gradient coefficient c increases from − 0.50 to 0.50 for $\alpha_0=1.0$. On the other hand, by increasing the mass ratio α_0, Ω_i ($i=1,2,3,4$) of the beam always decreases, irrespective of the value of the gradient coefficient. At the most sensitive state, increasing α_0 from 0.0 to 1.0 for $c=-0.50$ can reduce the quantity of Ω_1 for the NAFG beam in case 8 with $p=2$ by nearly 35%. Moreover, it should be noted that for the same conditions and regardless of the amount of the end mass ratio α_0, the natural frequencies of the NAFG cantilever beam with positive and negative gradient coefficient c always are greater and smaller than those of the uniform beam (i.e., $c=0$), respectively.

By observing data in Tables 13 and 14 and according to graphs in Figs. 13 and 14, it is found that as the NAFG parameters increase, Ω_i ($i=1,2,3,4$) for the NAFG cantilever beam always increases. This influence is more considerable whenever the gradient coefficient c increases. In other words, the effect of the gradient coefficient c on the natural frequencies of the NAFG cantilever beam is more significant than the gradient index p. On the other hand, changing the value of c in lower frequencies is considerable while changing the value of p in higher frequencies is significant, irrespective of the amount of the end mass ratio α_0. Furthermore, by increasing the mass ratio α_0, Ω_i ($i=1,2,3,4$) of NAFG cantilever beams always decreases, irrespective of the values of NAFG parameters. This effect is more pronounced for the first natural frequency.

Table 11 First four dimensionless natural frequency coefficients Ω_i, $i=1,2,3,4$ for Case 6

$\alpha_0=\alpha_L$	Ω_i	$T_0=T_L$					
		0.1	1	10	100	1000	10^5
0.0	$i=1$	0.680777	1.207542	2.094774	3.099660	3.430093	3.474321
	$i=2$	1.041079	1.848213	3.232774	5.154749	6.684785	7.000638
	$i=3$	5.305762	5.324498	5.510301	6.873084	9.438575	10.487663
	$i=4$	8.770339	8.774522	8.816701	9.260531	11.775333	13.966329
0.1	$i=1$	0.650530	1.154811	2.017931	3.074085	3.429569	3.474321
	$i=2$	0.972089	1.725778	3.017326	4.771797	6.626136	7.000632
	$i=3$	4.774292	4.788777	4.937985	6.210111	8.742497	10.487565
	$i=4$	8.036360	8.038684	8.062339	8.340163	10.593360	13.965591
0.2	$i=1$	0.625507	1.110931	1.950394	3.046400	3.429031	3.474321
	$i=2$	0.924606	1.641640	2.871557	4.484843	6.544850	7.000626
	$i=3$	4.498862	4.510484	4.633362	5.837992	8.115497	10.487464
	$i=4$	7.746795	7.748291	7.763555	7.949053	10.126346	13.964796
0.3	$i=1$	0.604393	1.073770	1.891058	3.016756	3.428479	3.474321
	$i=2$	0.888638	1.577986	2.763127	4.273803	6.435261	7.000620
	$i=3$	4.325815	4.335370	4.438146	5.575553	7.697244	10.487361
	$i=4$	7.587285	7.588331	7.598992	7.729037	9.809809	13.963937
0.4	$i=1$	0.586269	1.041791	1.838695	2.985415	3.427913	3.474321
	$i=2$	0.859755	1.526907	2.677116	4.115121	6.298961	7.000614
	$i=3$	4.205358	4.213356	4.300360	5.369509	7.434000	10.487255
	$i=4$	7.485145	7.485917	7.493775	7.588921	9.524159	13.963005
0.5	$i=1$	0.570480	1.013885	1.792184	2.952729	3.427331	3.474321
	$i=2$	0.835650	1.484291	2.605798	3.992803	6.147103	7.000607
	$i=3$	4.116014	4.122807	4.197236	5.199307	7.270122	10.487147
	$i=4$	7.413813	7.414406	7.420433	7.492607	9.258111	13.961990
0.6	$i=1$	0.556552	0.989238	1.750577	2.919114	3.426734	3.474321
	$i=2$	0.814981	1.447749	2.544788	3.896474	5.993145	7.000601
	$i=3$	4.046806	4.052648	4.116924	5.054622	7.165155	10.487037
	$i=4$	7.361063	7.361532	7.366298	7.422712	9.014844	13.960881
0.7	$i=1$	0.544134	0.967245	1.713096	2.885000	3.426120	3.474321
	$i=2$	0.796902	1.415781	2.491401	3.819208	5.845905	7.000595
	$i=3$	3.991466	3.996542	4.052528	4.929288	7.093693	10.486923
	$i=4$	7.320422	7.320803	7.324665	7.369870	8.795628	13.959661
0.8	$i=1$	0.532961	0.947443	1.679108	2.850794	3.425490	3.474321
	$i=2$	0.780846	1.387383	2.443893	3.756208	5.709138	7.000589
	$i=3$	3.946124	3.950575	3.999721	4.819213	7.041272	10.486807
	$i=4$	7.288129	7.288444	7.291637	7.328616	8.599363	13.958315
0.9	$i=1$	0.522830	0.929478	1.648100	2.816850	3.424841	3.474321
	$i=2$	0.766415	1.361852	2.401068	3.704039	5.583634	7.000582
	$i=3$	3.908248	3.912183	3.955631	4.721505	6.999833	10.486687
	$i=4$	7.261841	7.262106	7.264788	7.295570	8.423965	13.956819
1.0	$i=1$	0.513580	0.913069	1.619654	2.783454	3.424174	3.474321
	$i=2$	0.753318	1.338675	2.362073	3.660187	5.468872	7.000576
	$i=3$	3.876107	3.879610	3.918269	4.634032	6.964740	10.486565
	$i=4$	7.240019	7.240245	7.242530	7.268534	8.267199	13.955148

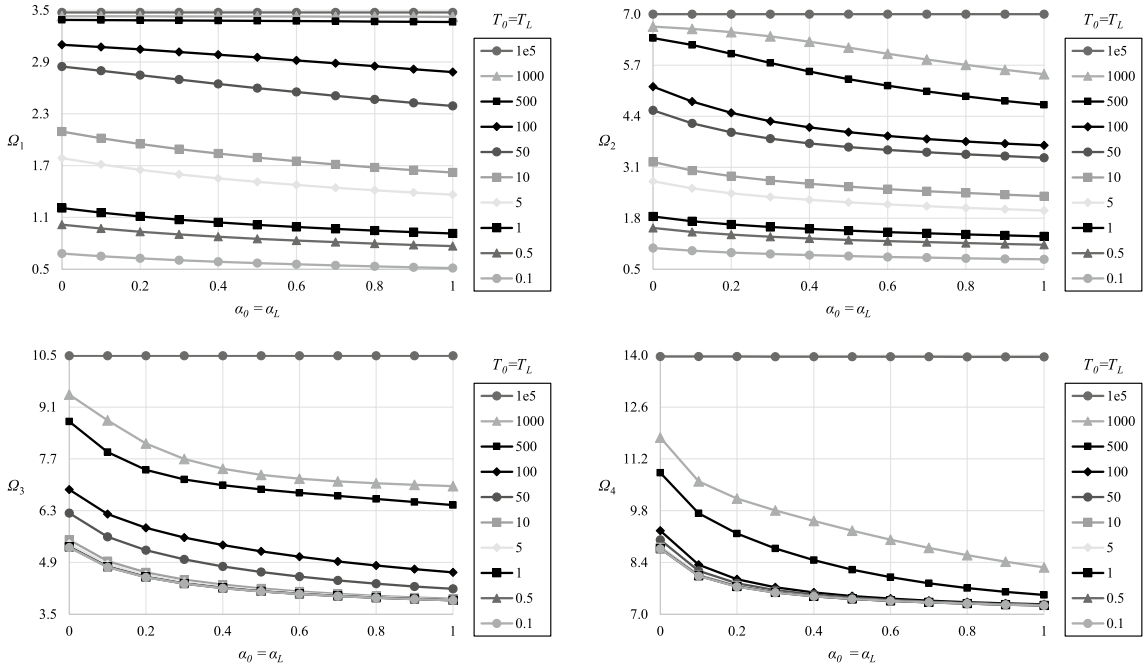

Fig. 11 Plot first four dimensionless natural frequency coefficients Ω_i, $i = 1,2,3,4$ for Case 6

Conclusion

The objective of this paper was to present the analytical solutions for investigating the free transverse vibration and obtaining the exact natural frequencies of the power-law NAFG beams with attached end point masses and general boundary conditions. In this way, based on the Euler–Bernoulli beam theory, the governing differential equation of motion was solved accurately using the Bessel functions. Then, the constant coefficients matrices of the power-law NAFG beams for $c > 0$, $c = 0$, and $c < 0$, with the end point masses and general elastic supports were derived

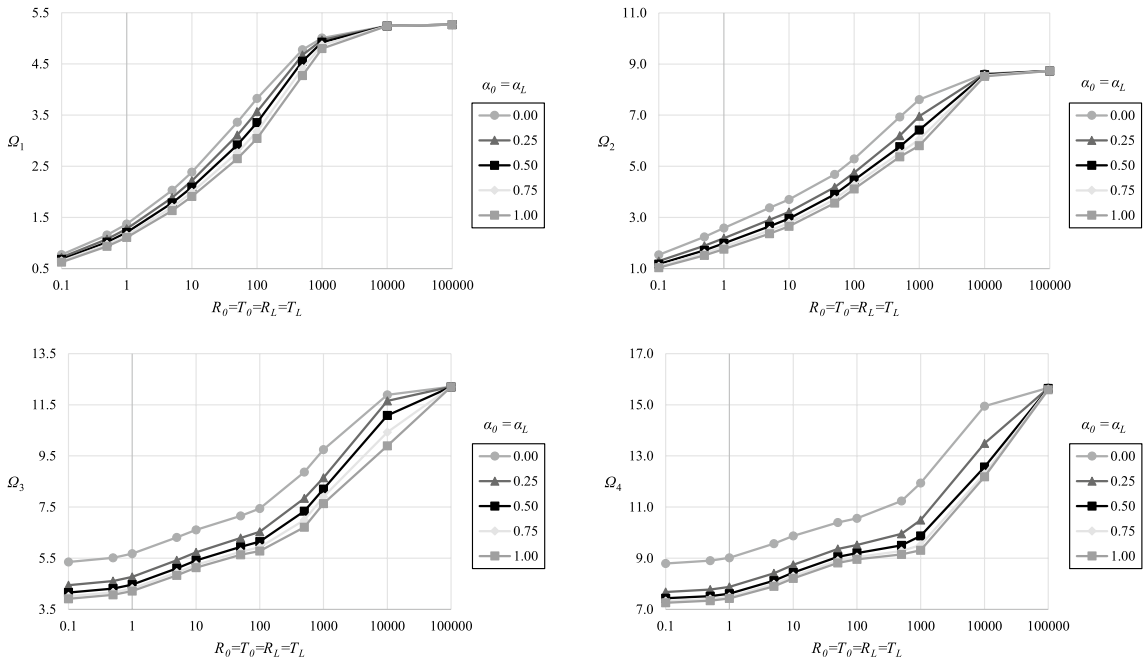

Fig. 12 Plot first four dimensionless natural frequency coefficients Ω_i, $i = 1,2,3,4$ for Case 7

Table 12 First four dimensionless natural frequency coefficients Ω_i, $i=1,2,3,4$ for Case 7

$\alpha_0=\alpha_L$	Ω_i	$R_0=T_0=R_L=T_L$					
		0.1	1	10	100	1000	10^5
0.00	$i=1$	0.773524	1.371950 [1.3719]*	2.387006 [2.3870]	3.824055	5.006038	5.268707
	$i=2$	1.541293	2.587009 [2.5870]	3.704935 [3.7049]	5.290770	7.608084	8.731475
	$i=3$	5.351114	5.681446 [5.6814]	6.608862 [6.6089]	7.445603	9.748147	12.204373
	$i=4$	8.798436	9.019529	9.873495	10.559896	11.940671	15.660438
0.25	$i=1$	0.720375	1.277536	2.216517	3.566550	4.971390	5.268703
	$i=2$	1.299723	2.190715	3.219908	4.755226	6.959969	8.731337
	$i=3$	4.448281	4.770599	5.731002	6.535237	8.648349	12.202910
	$i=4$	7.681547	7.877324	8.743987	9.520505	10.491938	15.651032
0.50	$i=1$	0.681463	1.208017	2.088795	3.352480	4.926971	5.268699
	$i=2$	1.177124	1.988217	2.958574	4.466989	6.420859	8.731196
	$i=3$	4.159542	4.472094	5.413675	6.149301	8.207496	12.201275
	$i=4$	7.436176	7.616372	8.443966	9.204906	9.870508	15.637810
0.75	$i=1$	0.651157	1.153790	1.989122	3.181165	4.870441	5.268695
	$i=2$	1.097318	1.856129	2.783973	4.270602	6.053366	8.731051
	$i=3$	4.010491	4.316276	5.242684	5.927737	7.898680	12.199436
	$i=4$	7.324667	7.496401	8.299499	9.048558	9.520583	15.617780
1.00	$i=1$	0.626553	1.109764	1.908565	3.042613	4.800680	5.268691
	$i=2$	1.039137	1.759635	2.654071	4.118094	5.804623	8.730902
	$i=3$	3.918310	4.219259	5.134389	5.784098	7.632208	12.197350
	$i=4$	7.260605	7.427087	8.213958	8.954983	9.313613	15.584018

*The values that are shown in square brackets are given by Bambaeechee [1]

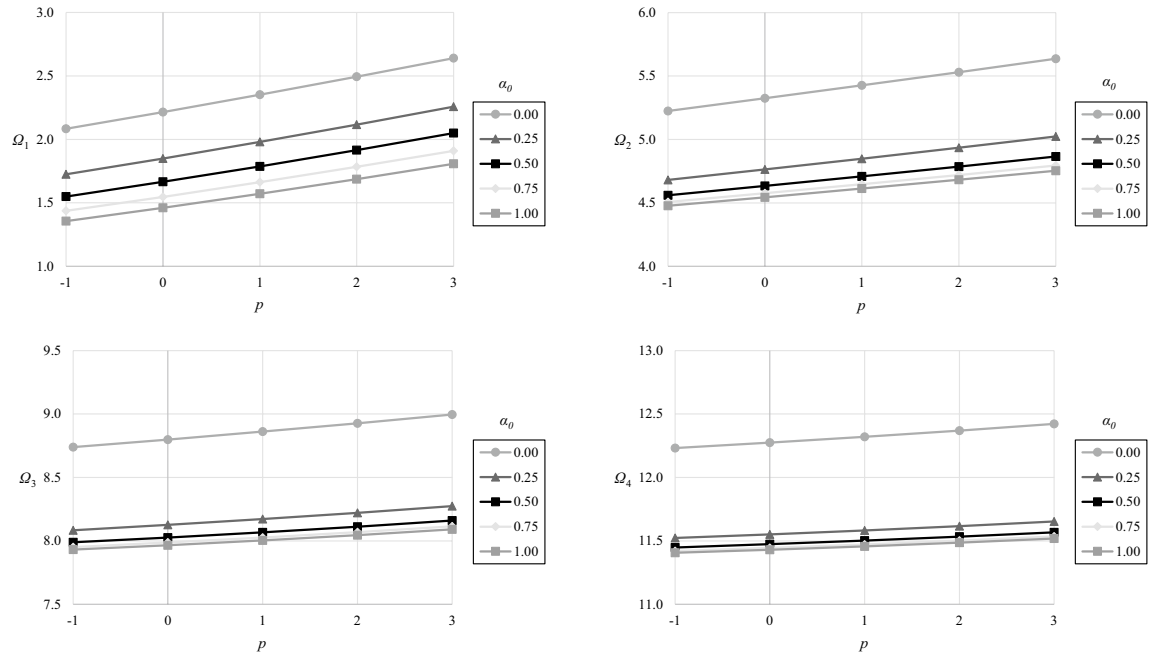

Fig. 13 Plot first four dimensionless natural frequency coefficients Ω_i, $i=1,2,3,4$ for Case 8 with $c=0.50$

by applying the boundary conditions. Accordingly, by taking the constant coefficients matrix determinant equal to zero and calculating the positive real roots, the natural frequencies were obtained. By comparing the responses of the numerical examples with the available solutions, the accuracy, capability, and efficiency of the proposed formulations were demonstrated. Subsequently, the effects of the attached end point masses, rotational and translational

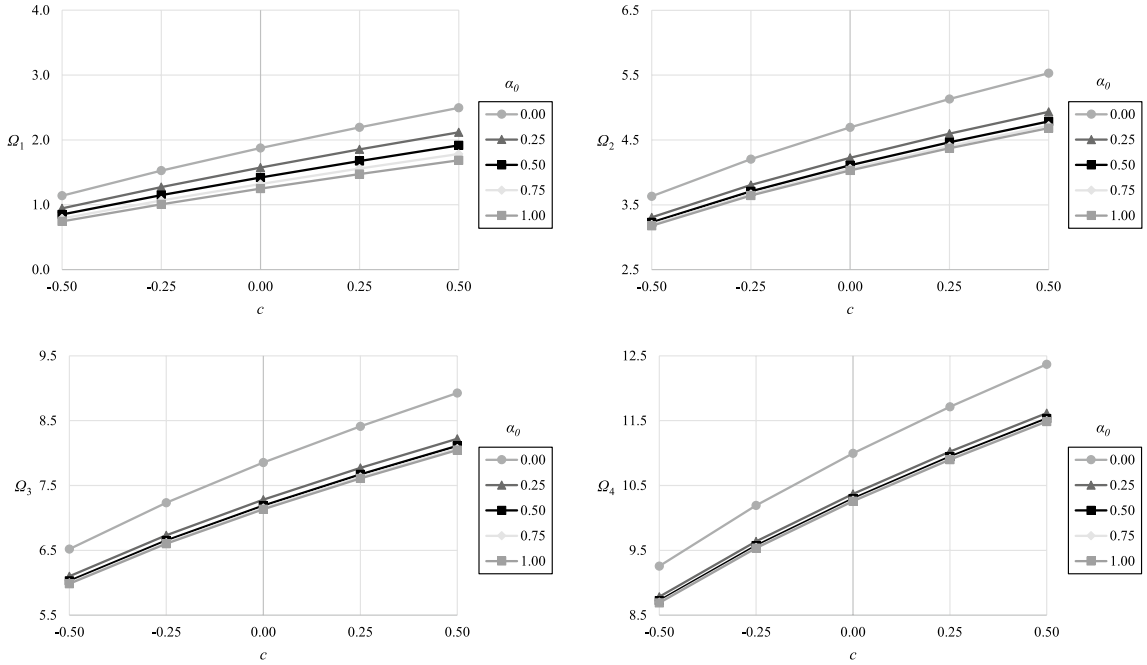

Fig. 14 Plot first four dimensionless natural frequency coefficients Ω_i, $i=1,2,3,4$ for Case 8 with $p=2$

Table 13 First four dimensionless natural frequency coefficients Ω_i, $i=1,2,3,4$ for Case 8 with $c=0.50$

α_0	Ω_i	P				
		− 1	0	1	2	3
0.00	$i=1$	2.083589	2.215475 [2.2155]*	2.352241 [2.3522]	2.493745 [2.4937]	2.639825 [2.6398]
	$i=2$	5.223767	5.324065 [5.3241]	5.426062 [5.4261]	5.529994 [5.5300]	5.636070 [5.6361]
	$i=3$	8.739036	8.798246 [8.7982]	8.860973 [8.8610]	8.927155 [8.9272]	8.996737 [8.9967]
	$i=4$	12.232411	12.275118	12.320909	12.369747	12.421594
0.25	$i=1$	1.724127	1.849107	1.979878	2.116313	2.258249
	$i=2$	4.681178	4.763829	4.848101	4.934337	5.022856
	$i=3$	8.083139	8.125680	8.171770	8.221368	8.274442
	$i=4$	11.522338	11.550527	11.581795	11.616114	11.653459
0.50	$i=1$	1.548651	1.665056	1.787305	1.915303	2.048915
	$i=2$	4.559890	4.633964	4.709299	4.786280	4.865273
	$i=3$	7.988474	8.026307	8.067584	8.112277	8.160364
	$i=4$	11.448197	11.473574	11.501983	11.533402	11.567810
0.75	$i=1$	1.436767	1.546570	1.662095	1.783264	1.909954
	$i=2$	4.506775	4.576647	4.647576	4.719973	4.794235
	$i=3$	7.951058	7.986929	8.026203	8.068854	8.114869
	$i=4$	11.420332	11.444620	11.471923	11.502221	11.535495
1.00	$i=1$	1.356280	1.460920	1.571131	1.686844	1.807944
	$i=2$	4.476988	4.544394	4.612733	4.682433	4.753914
	$i=3$	7.931038	7.965841	8.004023	8.045563	8.090453
	$i=4$	11.405734	11.429446	11.456165	11.485871	11.518547

*The values that are shown in square brackets are given by Bambaeechee [1]

Table 14 First four dimensionless natural frequency coefficients Ω_i, $i=1,2,3,4$ for Case 8 with $p=2$

α_0	Ω_i	c				
		− 0.50	− 0.25	0.00 (uniform)	0.25	0.50
0.00	$i=1$	1.139338	1.526994	1.875104 [1.8751]*	2.195198 [2.1952]	2.493745 [2.9437]
	$i=2$	3.631083	4.205135	4.694091 [4.6941]	5.130393 [5.1304]	5.529994 [5.5300]
	$i=3$	6.518745	7.233742	7.854757 [7.8548]	8.413556 [8.4136]	8.927155 [8.9272]
	$i=4$	9.257468	10.192160	10.995541	11.713400	12.369747
0.25	$i=1$	0.944366	1.273885	1.573751	1.852910	2.116313
	$i=2$	3.307288	3.805436	4.225113	4.596476	4.934337
	$i=3$	6.098766	6.733094	7.281236	7.772142	8.221368
	$i=4$	8.783626	9.638535	10.370450	11.022157	11.616114
0.50	$i=1$	0.849179	1.147515	1.419964	1.674438	1.915303
	$i=2$	3.230552	3.709456	4.111133	4.465226	4.786280
	$i=3$	6.029270	6.652292	7.190335	7.671889	8.112277
	$i=4$	8.724733	9.572638	10.298445	10.944603	11.533402
0.75	$i=1$	0.788319	1.066145	1.320266	1.557967	1.783264
	$i=2$	3.196233	3.666484	4.060080	4.406433	4.719973
	$i=3$	6.000970	6.619634	7.153811	7.631808	8.068854
	$i=4$	8.702001	9.547408	10.271046	10.915241	11.502221
1.00	$i=1$	0.744451	1.007290	1.247917	1.473178	1.686844
	$i=2$	3.176777	3.642120	4.031139	4.373123	4.682433
	$i=3$	5.985624	6.601987	7.134132	7.610264	8.045563
	$i=4$	8.689959	9.534090	10.256621	10.899816	11.485871

*The values that are shown in square brackets are given by Bambaeechee [1]

elastic supports, and NAFG parameters on the values of the first four natural frequencies of the power-law NAFG beams for the eight parametric cases were studied comprehensively. The analytical solutions were presented in tabular and graphical forms and could be used as either the benchmark problems or proper design of the composite beams with attached end point masses and general boundary conditions.

Based on the results of this research, the following important points are concluded:

- As the end point mass ratios increase, the natural frequencies of the power-law NAFG beam decrease. Among the cases studied, the natural frequency of the beam can reduce by up to 33% when the end point mass ratios increase.
- The natural frequencies of the power-law NAFG beam increase, as the stiffness ratios increase. Among the cases studied, the natural frequency of the beam can rise by up to 9.3 times, when the stiffness ratios increase.
- According to the slope of the Ω-α curves, the mass sensitivity differs from one power-law NAFG beam to another, and from one mode of vibration to another.
- The sensitivity of the natural frequencies of the beam to the variation of the translational stiffness ratios is greater than the rotational stiffness ratios.
- As the power-law NAFG parameters increase, the natural frequencies of the cantilever beam increase. Nevertheless, the effect of the gradient coefficient c on the natural frequencies of the beam is more significant than the gradient index p.

Appendix A

For the derivation of the general solution Eq. (9), the compact form of the differential equation obtained in Eq. (8), according to Eq. (4), can be expressed as follows [67]:

$$\frac{d^2}{\mathrm{d}X^2}\left[X^{p+2}\frac{d^2W_i(X)}{\mathrm{d}X^2}\right]-\frac{\Omega_i^4}{c^4}X^pW_i(X)=0. \tag{28}$$

Eq. (28) can be factored into:

$$\left[X^{-p}\frac{d}{\mathrm{d}X}\left(X^{p+1}\frac{d}{\mathrm{d}X}\right)+\frac{\Omega_i^2}{c^2}\right]\left[X^{-p}\frac{d}{\mathrm{d}X}\left(X^{p+1}\frac{d}{\mathrm{d}X}\right)-\frac{\Omega_i^2}{c^2}\right]W_i(X)=0. \tag{29}$$

Each one of the brackets in Eq. (29) is a Bessel operator. One can find the general solution of $W_i(X)$ as:

$$W_i(X)=A_i(X)+B_i(X), \tag{30}$$

where

$$\left[X^{-p}\frac{d}{\mathrm{d}X}\left(X^{p+1}\frac{d}{\mathrm{d}X}\right)+\frac{\Omega_i^2}{c^2}\right]A_i(X)=0, \tag{31}$$

$$\left[X^{-p}\frac{d}{\mathrm{d}X}\left(X^{p+1}\frac{d}{\mathrm{d}X}\right)-\frac{\Omega_i^2}{c^2}\right]B_i(X)=0. \tag{32}$$

The Eq. (31) is the regular Bessel differential equation, and the solution can be written as:

$$A_i(X)=X^{-\frac{p}{2}}\left[C_1J_p\left(\frac{2\Omega_i\sqrt{X}}{c}\right)+C_2Y_p\left(\frac{2\Omega_i\sqrt{X}}{c}\right)\right], \tag{33}$$

where C_1 and C_2 are unknown constants, and J_p and Y_p are, respectively, the Bessel functions of first and second kinds of order p. The Eq. (32) is known as the modified Bessel differential equation, and the solution can be expressed as:

$$B_i(X)=X^{-\frac{p}{2}}\left[C_3I_p\left(\frac{2\Omega_i\sqrt{X}}{c}\right)+C_4K_p\left(\frac{2\Omega_i\sqrt{X}}{c}\right)\right], \tag{34}$$

where C_3 and C_4 are unknown constants, and I_p and K_p are, respectively, the modified Bessel functions of first and second kinds of order p. Therefore, the general solution of $W_i(X)$ according to Eq. (30) is:

$$\begin{aligned}W_i(X)=X^{-\frac{p}{2}}&\left[C_1J_p\left(\frac{2\Omega_i\sqrt{X}}{c}\right)+C_2Y_p\left(\frac{2\Omega_i\sqrt{X}}{c}\right)\right.\\&\left.+C_3I_p\left(\frac{2\Omega_i\sqrt{X}}{c}\right)+C_4K_p\left(\frac{2\Omega_i\sqrt{X}}{c}\right)\right].\end{aligned} \tag{35}$$

Appendix B

The elements of the constant coefficients matrix, **A** for the NAFG beams with the positive gradient coefficient (i.e., $c>0$), carrying tip masses and various elastic boundary conditions are as follows:

$$A_{11}=-\Omega J_p\left(\frac{2\Omega}{c}\right)+\left[R_0+c(p+1)\right]J_{p+1}\left(\frac{2\Omega}{c}\right), \tag{36}$$

$$A_{12}=-\Omega Y_p\left(\frac{2\Omega}{c}\right)+\left[R_0+c(p+1)\right]Y_{p+1}\left(\frac{2\Omega}{c}\right), \tag{37}$$

$$A_{13}=\Omega I_p\left(\frac{2\Omega}{c}\right)-\left[R_0+c(p+1)\right]I_{p+1}\left(\frac{2\Omega}{c}\right), \tag{38}$$

$$A_{14}=\Omega K_p\left(\frac{2\Omega}{c}\right)+\left[R_0+c(p+1)\right]K_{p+1}\left(\frac{2\Omega}{c}\right), \tag{39}$$

$$A_{21}=\left(T_0-\alpha_0\Omega^4\right)J_p\left(\frac{2\Omega}{c}\right)+\Omega^3J_{p+1}\left(\frac{2\Omega}{c}\right), \tag{40}$$

$$A_{22}=\left(T_0-\alpha_0\Omega^4\right)Y_p\left(\frac{2\Omega}{c}\right)+\Omega^3Y_{p+1}\left(\frac{2\Omega}{c}\right), \tag{41}$$

$$A_{23}=\left(T_0-\alpha_0\Omega^4\right)I_p\left(\frac{2\Omega}{c}\right)+\Omega^3I_{p+1}\left(\frac{2\Omega}{c}\right), \tag{42}$$

$$A_{24}=\left(T_0-\alpha_0\Omega^4\right)K_p\left(\frac{2\Omega}{c}\right)-\Omega^3K_{p+1}\left(\frac{2\Omega}{c}\right), \tag{43}$$

$$\begin{aligned}A_{31}=&-\Omega\sqrt{1+c}J_p\left(\frac{2\Omega\sqrt{1+c}}{c}\right)\\&-\left[R_L(1+c)-c(p+1)\right]J_{p+1}\left(\frac{2\Omega\sqrt{1+c}}{c}\right),\end{aligned} \tag{44}$$

$$\begin{aligned}A_{32}=&-\Omega\sqrt{1+c}Y_p\left(\frac{2\Omega\sqrt{1+c}}{c}\right)\\&-\left[R_L(1+c)-c(p+1)\right]Y_{p+1}\left(\frac{2\Omega\sqrt{1+c}}{c}\right),\end{aligned} \tag{45}$$

$$\begin{aligned}A_{33}=&\Omega\sqrt{1+c}I_p\left(\frac{2\Omega\sqrt{1+c}}{c}\right)\\&+\left[R_L(1+c)-c(p+1)\right]I_{p+1}\left(\frac{2\Omega\sqrt{1+c}}{c}\right),\end{aligned} \tag{46}$$

$$\begin{aligned}A_{34}=&\Omega\sqrt{1+c}K_p\left(\frac{2\Omega\sqrt{1+c}}{c}\right)\\&-\left[R_L(1+c)-c(p+1)\right]K_{p+1}\left(\frac{2\Omega\sqrt{1+c}}{c}\right),\end{aligned} \tag{47}$$

$$\begin{aligned}A_{41}=&\left[-T_L(1+c)^{p+2}+\alpha_L\Omega^4\right]J_p\left(\frac{2\Omega\sqrt{1+c}}{c}\right)\\&+\Omega^3(1+c)^{p+\frac{1}{2}}J_{p+1}\left(\frac{2\Omega\sqrt{1+c}}{c}\right),\end{aligned} \tag{48}$$

$$\begin{aligned}A_{42}=&\left[-T_L(1+c)^{p+2}+\alpha_L\Omega^4\right]Y_p\left(\frac{2\Omega\sqrt{1+c}}{c}\right)\\&+\Omega^3(1+c)^{p+\frac{1}{2}}Y_{p+1}\left(\frac{2\Omega\sqrt{1+c}}{c}\right),\end{aligned} \tag{49}$$

$$A_{43} = \left[-T_L(1+c)^{p+2} + \alpha_L\Omega^4\right] I_p\left(\frac{2\Omega\sqrt{1+c}}{c}\right) + \Omega^3(1+c)^{p+\frac{1}{2}} I_{p+1}\left(\frac{2\Omega\sqrt{1+c}}{c}\right), \tag{50}$$

$$A_{44} = \left[-T_L(1+c)^{p+2} + \alpha_L\Omega^4\right] K_p\left(\frac{2\Omega\sqrt{1+c}}{c}\right) - \Omega^3(1+c)^{p+\frac{1}{2}} K_{p+1}\left(\frac{2\Omega\sqrt{1+c}}{c}\right). \tag{51}$$

For the uniform beam, i.e., $c = 0$, the entries of the unknown constants' matrix, **A** are as below:

$$A_{11} = -R_0 \tag{52}$$

$$A_{12} = -\Omega \tag{53}$$

$$A_{13} = -R_0 \tag{54}$$

$$A_{14} = \Omega \tag{55}$$

$$A_{21} = -\Omega^3 \tag{56}$$

$$A_{22} = T_0 - \alpha_0\Omega^4 \tag{57}$$

$$A_{23} = \Omega^3 \tag{58}$$

$$A_{24} = T_0 - \alpha_0\Omega^4 \tag{59}$$

$$A_{31} = -\Omega\sin(\Omega) + R_L\cos(\Omega) \tag{60}$$

$$A_{32} = -\Omega\cos(\Omega) - R_L\sin(\Omega) \tag{61}$$

$$A_{33} = \Omega\sinh(\Omega) + R_L\cosh(\Omega) \tag{62}$$

$$A_{34} = \Omega\cosh(\Omega) + R_L\sinh(\Omega) \tag{63}$$

$$A_{41} = (-T_L + \alpha_L\Omega^4)\sin(\Omega) - \Omega^3\cos(\Omega) \tag{64}$$

$$A_{42} = (-T_L + \alpha_L\Omega^4)\cos(\Omega) + \Omega^3\sin(\Omega) \tag{65}$$

$$A_{43} = (-T_L + \alpha_L\Omega^4)\sinh(\Omega) + \Omega^3\cosh(\Omega) \tag{66}$$

$$A_{44} = (-T_L + \alpha_L\Omega^4)\cosh(\Omega) + \Omega^3\sinh(\Omega) \tag{67}$$

The elements of the constant coefficients matrix, **A** for the NAFG beams with the negative gradient coefficient (i.e., $-1 < c < 0$), carrying tip masses and general elastic boundary conditions are as follows:

$$A_{11} = -\Omega J_p\left(-\frac{2\Omega}{c}\right) - \left[R_0 + c(p+1)\right] J_{p+1}\left(-\frac{2\Omega}{c}\right) \tag{68}$$

$$A_{12} = -\Omega Y_p\left(-\frac{2\Omega}{c}\right) - \left[R_0 + c(p+1)\right] Y_{p+1}\left(-\frac{2\Omega}{c}\right) \tag{69}$$

$$A_{13} = \Omega I_p\left(-\frac{2\Omega}{c}\right) + \left[R_0 + c(p+1)\right] I_{p+1}\left(-\frac{2\Omega}{c}\right) \tag{70}$$

$$A_{14} = \Omega K_p\left(-\frac{2\Omega}{c}\right) - \left[R_0 + c(p+1)\right] K_{p+1}\left(-\frac{2\Omega}{c}\right) \tag{71}$$

$$A_{21} = \left(T_0 - \alpha_0\Omega^4\right) J_p\left(-\frac{2\Omega}{c}\right) - \Omega^3 J_{p+1}\left(-\frac{2\Omega}{c}\right) \tag{72}$$

$$A_{22} = \left(T_0 - \alpha_0\Omega^4\right) Y_p\left(-\frac{2\Omega}{c}\right) - \Omega^3 Y_{p+1}\left(-\frac{2\Omega}{c}\right) \tag{73}$$

$$A_{23} = \left(T_0 - \alpha_0\Omega^4\right) I_p\left(-\frac{2\Omega}{c}\right) - \Omega^3 I_{p+1}\left(-\frac{2\Omega}{c}\right) \tag{74}$$

$$A_{24} = \left(T_0 - \alpha_0\Omega^4\right) K_p\left(-\frac{2\Omega}{c}\right) + \Omega^3 K_{p+1}\left(-\frac{2\Omega}{c}\right) \tag{75}$$

$$A_{31} = -\Omega\sqrt{1+c} J_p\left(-\frac{2\Omega\sqrt{1+c}}{c}\right) + \left[R_L(1+c) - c(p+1)\right] J_{p+1}\left(-\frac{2\Omega\sqrt{1+c}}{c}\right) \tag{76}$$

$$A_{32} = -\Omega\sqrt{1+c} Y_p\left(-\frac{2\Omega\sqrt{1+c}}{c}\right) + \left[R_L(1+c) - c(p+1)\right] Y_{p+1}\left(-\frac{2\Omega\sqrt{1+c}}{c}\right) \tag{77}$$

$$A_{33} = \Omega\sqrt{1+c} I_p\left(-\frac{2\Omega\sqrt{1+c}}{c}\right) - \left[R_L(1+c) - c(p+1)\right] I_{p+1}\left(-\frac{2\Omega\sqrt{1+c}}{c}\right) \tag{78}$$

$$A_{34} = \Omega\sqrt{1+c}K_p\left(-\frac{2\Omega\sqrt{1+c}}{c}\right) + \left[R_L(1+c) - c(p+1)\right]K_{p+1}\left(-\frac{2\Omega\sqrt{1+c}}{c}\right) \quad (79)$$

$$A_{41} = \left[-T_L(1+c)^{p+2} + \alpha_L\Omega^4\right]J_p\left(-\frac{2\Omega\sqrt{1+c}}{c}\right) - \Omega^3(1+c)^{p+\frac{1}{2}}J_{p+1}\left(-\frac{2\Omega\sqrt{1+c}}{c}\right) \quad (80)$$

$$A_{42} = \left[-T_L(1+c)^{p+2} + \alpha_L\Omega^4\right]Y_p\left(-\frac{2\Omega\sqrt{1+c}}{c}\right) - \Omega^3(1+c)^{p+\frac{1}{2}}Y_{p+1}\left(-\frac{2\Omega\sqrt{1+c}}{c}\right) \quad (81)$$

$$A_{43} = \left[-T_L(1+c)^{p+2} + \alpha_L\Omega^4\right]I_p\left(-\frac{2\Omega\sqrt{1+c}}{c}\right) - \Omega^3(1+c)^{p+\frac{1}{2}}I_{p+1}\left(-\frac{2\Omega\sqrt{1+c}}{c}\right) \quad (82)$$

$$A_{44} = \left[-T_L(1+c)^{p+2} + \alpha_L\Omega^4\right]K_p\left(-\frac{2\Omega\sqrt{1+c}}{c}\right) + \Omega^3(1+c)^{p+\frac{1}{2}}K_{p+1}\left(-\frac{2\Omega\sqrt{1+c}}{c}\right). \quad (83)$$

Funding The author received no financial support for the research, authorship, and/or publication of this article.

Declarations

Conflict of interest The author declared no potential conflicts of interest with respect to the research, authorship, and/or publication of this article.

References

1. Bambaeechee M (2019) Free vibration of AFG beams with elastic end restraints. Steel Compos Struct 33:403–432
2. Mabie HH, Rogers CB (1964) Transverse vibrations of tapered cantilever beams with end loads. J Acoust Soc Am 36:463–469
3. Mabie HH, Rogers CB (1974) Transverse vibrations of double-tapered cantilever beams with end support and with end mass. J Acoust Soc Am 55:986–991
4. Sankaran GV, Kanaka Raju K, Venkateswara Rao G (1975) Vibration frequencies of a tapered beam with one end spring-hinged and carrying a mass at the other free end. J Appl Mech 42:740–741
5. Goel RP (1976) Transverse vibrations of tapered beams. J Sound Vib 47:1–7
6. Lee TW (1976) Transverse vibrations of a tapered beam carrying a concentrated mass. J Appl Mech 43:366–367
7. Lau JH (1984) Vibration frequencies of tapered bars with end mass. J Appl Mech 51:179–181
8. Lau JH (1984) Vibration frequencies for a non-uniform beam with end mass. J Sound Vib 97:513–521
9. Laura PAA, Gutierrez RH (1986) Vibrations of an elastically restrained cantilever beam of varying cross section with tip mass of finite length. J Sound Vib 108:123–131
10. Alvarez SI, Ficcadenti de Iglesias GM, Laura PAA (1988) Vibrations of an elastically restrained, non-uniform beam with translational and rotational springs, and with a tip mass. J Sound Vib 120:465–471
11. Yang KY (1990) The natural frequencies of a non-uniform beam with a tip mass and with translational and rotational springs. J Sound Vib 137:339–341
12. Rossi RE, Laura PAA, Gutierrez RH (1990) A note on transverse vibrations of a Timoshenko beam of non-uniform thickness clamped at one end and carrying a concentrated mass at the other. J Sound Vib 143:491–502
13. Lee SY, Lin SM (1992) Exact vibration solutions for nonuniform Timoshenko beams with attachments. AIAA J 30:2930–2934
14. Matsuda H, Morita C, Sakiyama T (1992) A method for vibration analysis of a tapered timoshenko beam with constraint at any points and carrying a heavy tip body. J Sound Vib 158:331–339
15. Grossi RO, Aranda A, Bhat RB (1993) Vibration of tapered beams with one end spring hinged and the other end with tip mass. J Sound Vib 160:175–178
16. Auciello NM (1996) LETTER TO THE EDITOR: Free vibrations of a linearly tapered cantilever beam with constraining springs and tip mass. J Sound Vib 192:905–911
17. Auciello NM (1996) Transverse vibrations of a linearly tapered cantilever beam with tip mass of rotary inertia and eccentricity. J Sound Vib 194:25–34
18. Auciello NM, Maurizi MJ (1997) On the natural vibrations of tapered beams with attached inertia elements. J Sound Vib 199:522–530
19. Auciello NM, Nolè G (1998) Vibrations of a cantilever tapered beam with varying section properties and carrying a mass at the free end. J Sound Vib 214:105–119
20. Wu J, Hsieh M (2000) Free vibration analysis of a non-uniform beam with multiple point masses. Struct Eng Mech 9:449–467
21. Li QS (2000) An exact approach for free flexural vibrations of multistep nonuniform beams. J Vib Control 6:963–983
22. Li QS (2002) Free vibration analysis of non-uniform beams with an arbitrary number of cracks and concentrated masses. J Sound Vib 252:509–525
23. Chen D-W, Wu J-S (2002) The exact solutions for the natural frequencies and mode shapes of non-uniform beams with multiple spring-mass systems. J Sound Vib 255:299–322
24. Karami G, Malekzadeh P, Shahpari SA (2003) A DQEM for vibration of shear deformable nonuniform beams with general boundary conditions. Eng Struct 25:1169–1178
25. Wu J-S, Chen D-W (2003) Bending vibrations of wedge beams with any number of point masses. J Sound Vib 262:1073–1090
26. Wu J-S, Chiang L-K (2004) Free vibrations of solid and hollow wedge beams with rectangular or circular cross-sections and carrying any number of point masses. Int J Numer Methods Eng 60:695–718
27. De Rosa MA, Maurizi MJ (2005) Damping in exact analysis of tapered beams. J Sound Vib 286:1041–1047

28. Wu J-S, Chen C-T (2005) An exact solution for the natural frequencies and mode shapes of an immersed elastically restrained wedge beam carrying an eccentric tip mass with mass moment of inertia. J Sound Vib 286:549–568
29. Chen D-W, Liu T-L (2006) Free and forced vibrations of a tapered cantilever beam carrying multiple point masses. Struct Eng Mech 23:209–216
30. Lai H-Y, Chen C-K, Hsu J-C (2008) Free vibration of non-uniform Euler-Bernoulli beams by the Adomian modified decomposition method. CMES - Comput Model Eng Sci 34:87–115
31. Lin H-Y (2010) An exact solution for free vibrations of a non-uniform beam carrying multiple elastic-supported rigid bars. Struct Eng Mech 34:399–416
32. Attarnejad R, Shahba A, Eslaminia M (2011) Dynamic basic displacement functions for free vibration analysis of tapered beams. J Vib Control 17:2222–2238
33. Firouz-Abadi RD, Rahmanian M, Amabili M (2013) Exact solutions for free vibrations and buckling of double tapered columns with elastic foundation and tip mass. J Vib Acoust 135:051017-1–51110
34. Wang CY (2013) Vibration of a tapered cantilever of constant thickness and linearly tapered width. Arch Appl Mech 83:171–176
35. Malaeke H, Moeenfard H (2016) Analytical modeling of large amplitude free vibration of non-uniform beams carrying a both transversely and axially eccentric tip mass. J Sound Vib 366:211–229
36. Sagar Singh S, Pal P, Kumar Pandey A (2016) Mass sensitivity of nonuniform microcantilever beams. J Vib Acoust 138
37. Nikolić A, Šalinić S (2017) A rigid multibody method for free vibration analysis of beams with variable axial parameters. J Vib Control 23:131–146
38. Torabi K, Afshari H, Sadeghi M et al (2017) Exact closed-form solution for vibration analysis of truncated conical and tapered beams carrying multiple concentrated masses. J Solid Mech 9:760–782
39. Huang CA, Wu JS, Shaw H-J (2018) Free vibration analysis of a nonlinearly tapered beam carrying arbitrary concentrated elements by using the continuous-mass transfer matrix method. J Mar Sci Technol Taiwan 26:28–49
40. Hsu CP, Hung CF, Liao JY (2018) Shock and Vibration, A Chebyshev spectral method with null space approach for boundary-value problems of Euler-Bernoulli beam, 2018. Available from: https://www.hindawi.com/journals/sv/2018/2487697/.
41. Elishakoff I, Johnson V (2005) Apparently the first closed-form solution of vibrating inhomogeneous beam with a tip mass. J Sound Vib 286:1057–1066
42. Elishakoff I, Perez A (2005) Design of a polynomially inhomogeneous bar with a tip mass for specified mode shape and natural frequency. J Sound Vib 287:1004–1012
43. Huang Y, Li X-F (2010) A new approach for free vibration of axially functionally graded beams with non-uniform cross-section. J Sound Vib 329:2291–2303
44. De Rosa MA, Lippiello M, Maurizi MJ et al (2010) Free vibration of elastically restrained cantilever tapered beams with concentrated viscous damping and mass. Mech Res Commun 37:261–264
45. Shahba A, Attarnejad R, Marvi MT et al (2011) Free vibration and stability analysis of axially functionally graded tapered Timoshenko beams with classical and non-classical boundary conditions. Compos Part B Eng 42:801–808
46. Wang CY, Wang CM (2012) Exact vibration solution for exponentially tapered cantilever with tip mass. J Vib Acoust 134:041012-1–41014
47. Li X-F, Kang Y-A, Wu J-X (2013) Exact frequency equations of free vibration of exponentially functionally graded beams. Appl Acoust 74:413–420
48. Li XF (2013) Free vibration of axially loaded shear beams carrying elastically restrained lumped-tip masses via asymptotic Timoshenko beam theory. J Eng Mech 139:418–428
49. Zhang H, Kang YA, Li X-F (2013) Stability and vibration analysis of axially-loaded shear beam-columns carrying elastically restrained mass. Appl Math Model 37:8237–8250
50. Tang A-Y, Wu J-X, Li X-F et al (2014) Exact frequency equations of free vibration of exponentially non-uniform functionally graded Timoshenko beams. Int J Mech Sci 89:1–11
51. Tang H-L, Shen Z-B, Li D-K (2014) Vibration of nonuniform carbon nanotube with attached mass via nonlocal Timoshenko beam theory. J Mech Sci Technol 28:3741–3747
52. Yuan J, Pao Y-H, Chen W (2016) Exact solutions for free vibrations of axially inhomogeneous Timoshenko beams with variable cross section. Acta Mech 227:2625–2643
53. Chen DQ, Sun DL, Li XF (2017) Surface effects on resonance frequencies of axially functionally graded Timoshenko nanocantilevers with attached nanoparticle. Compos Struct 173:116–126
54. Rahmani O, Mohammadi Niaei A, Hosseini SAH et al (2017) In-plane vibration of FG micro/nano-mass sensor based on nonlocal theory under various thermal loading via differential transformation method. Superlattices Microstruct 101:23–39
55. Nikolić A (2017) Free vibration analysis of a non-uniform axially functionally graded cantilever beam with a tip body. Arch Appl Mech 87:1227–1241
56. Rossit CA, Bambill DV, Gilardi GJ (2017) Free vibrations of AFG cantilever tapered beams carrying attached masses. Struct Eng Mech 61:685–691
57. Ghadiri M, Jafari A (2018) A nonlocal first order shear deformation theory for vibration analysis of size dependent functionally graded nano beam with attached tip mass: an exact solution. J Solid Mech 10:23–37
58. Šalinić S, Obradović A, Tomović A (2018) Free vibration analysis of axially functionally graded tapered, stepped, and continuously segmented rods and beams. Compos Part B Eng 150:135–143
59. Rossit CA, Bambill DV, Gilardi GJ (2018) Timoshenko theory effect on the vibration of axially functionally graded cantilever beams carrying concentrated masses. Struct Eng Mech 66:703–711
60. Mahmoud MA (2019) Natural frequency of axially functionally graded, tapered cantilever beams with tip masses. Eng Struct 187:34–42
61. Sun D-L, Li X-F (2019) Initial value method for free vibration of axially loaded functionally graded Timoshenko beams with nonuniform cross section. Mech Based Des Struct Mach 47:102–120
62. Nguyen KV, Dao TTB, Van Cao M (2020) Comparison studies of the receptance matrices of the isotropic homogeneous beam and the axially functionally graded beam carrying concentrated masses. Appl Acoust 160:107160
63. Li Z, Xu Y, Huang D (2021) Analytical solution for vibration of functionally graded beams with variable cross-sections resting on Pasternak elastic foundations. Int J Mech Sci 191:106084
64. Sahu RP, Sutar MK, Pattnaik S (2022) A generalized finite element approach to thefree vibration analysis of non-uniform axially functionally graded beam Scientia Iranica B 29(2):556–571
65. Liu X, Chang L, Banerjee JR et al (2022) Closed-form dynamic stiffness formulation for exact modal analysis of tapered and functionally graded beams and their assemblies. Int J Mech Sci 214:106887
66. Rao SS (2019) Vibration of Continuous Systems. John Wiley & Sons Inc
67. Wang CY, Wang CM (2013) Structural Vibration: Exact Solutions for Strings, Membranes, Beams, and Plates. Florida, CRC Press, Boca Raton
68. Watson GN (1995) A Treatise on the Theory of Bessel Functions. Cambridge University Press

69. Çelik İ (2018) Free vibration of non-uniform Euler-Bernoulli beam under various supporting conditions using Chebyshev wavelet collocation method. Appl Math Model 54:268–280
70. Mao Q (2011) Free vibration analysis of multiple-stepped beams by using Adomian decomposition method. Math Comput Model 54:756–764
71. Hsu J-C, Lai H-Y, Chen CK (2008) Free vibration of non-uniform Euler-Bernoulli beams with general elastically end constraints using Adomian modified decomposition method. J Sound Vib 318:965–981
72. De Rosa MA, Auciello NM (1996) Free vibrations of tapered beams with flexible ends. Comput Struct 60:197–202